



Published in final edited form as:

*Ind Eng Chem Res.* 2015 April 29; 54(16): 4043–4059. doi:10.1021/ie504452j.

## Emergence and Utility of Nonspherical Particles in Biomedicine

Margaret B. Fish<sup>1</sup>, Alex J. Thompson<sup>1</sup>, Catherine A. Fromen<sup>1</sup>, and Omolola Eniola-Adefeso<sup>1,\*</sup>

<sup>1</sup>Department of Chemical Engineering, University of Michigan, 2800 Plymouth Rd, NCRC B28-G102E, Ann Arbor, MI 48109, USA

### Abstract

The importance of the size of targeted, spherical drug carriers has been previously explored and reviewed. Particle shape has emerged as an equally important parameter in determining the *in vivo* journey and efficiency of drug carrier systems. Researchers have invented techniques to better control the geometry of particles of many different materials, which have allowed for exploration of the role of particle geometry in the phases of drug delivery. The important biological processes include clearance by the immune system, trafficking to the target tissue, margination to the endothelial surface, interaction with the target cell, and controlled release of a payload. The review of current literature herein supports that particle shape can be altered to improve a system's targeting efficiency. Non-spherical particles can harness the potential of targeted drug carriers by enhancing targeted site accumulation while simultaneously decreasing side effects and mitigating some limitations faced by spherical carriers.

### Keywords

Particle shape; Hemodynamics; Non-spherical drug carrier; Immune clearance; Margination; Biodistribution; Cellular internalization; Drug release

### Introduction

The design of new drug delivery systems has garnered significant attention in recent decades with the goal to greatly improve the treatment and diagnosis of major diseases including cancer and atherosclerosis.<sup>1,2</sup> Systemic administration of small molecule pharmaceutical treatments results in undirected distribution of the therapeutic throughout the body. This leads to unnecessary delivery to healthy cells, resulting in potentially severe side effects that trigger dose-limiting toxicity.<sup>3</sup> To overcome the non-specific delivery of such therapeutics, particulate drug delivery systems ranging in size from a few nanometers to a few microns have been designed to specifically accumulate in the diseased tissue of interest, simultaneously increasing the local concentration and efficacy of the drug while decreasing systemic side effects.<sup>4</sup>

\*Corresponding Author. lolaa@umich.edu.

#### Conflict of Interest Disclosure

The authors declare no competing conflict of interest.

The change in scale from a molecular therapeutic to a relatively large particle creates new opportunities to improve drug efficiency and specificity. The loading of drug cargo into or onto particle carriers<sup>5</sup> improves upon freely soluble systems by protecting the cargo from enzymatic degradation while providing controlled, sustained release. Unlike small molecule drugs, most particle systems are physically unable to pass through the tight junctions of endothelial cells (ECs) to the surrounding tissue, limiting their exposure to healthy cells.<sup>6</sup> This incapacity to extravasate out of the blood stream can be harnessed to treat specific disease conditions. Particles are restricted to the circulatory system, subsequently increasing exposure to the vasculature and ECs. Conjugating ligands to the surface of particles can actively target diseased ECs. These ligands have high specificity to cellular surface proteins involved in specific disease pathophysiology.<sup>4,7</sup> With cancer, the tight cellular junctions near tumors are disrupted, resulting in a leaky vasculature that allows intravenously delivered particles to passively accumulate through the enhanced permeability and retention (EPR) effect.<sup>8</sup>

The change in scale has revealed new biological hurdles for particulate carriers that were not previously encountered by small molecule drugs.<sup>9</sup> Injected particles face physical barriers throughout the body including filtration by the spleen, liver, and kidney, which restrict passage of particles of varying sizes. Particle carriers are an ideal size to interact with the reticuloendothelial system (RES), a network of phagocytic cells such as monocytes and macrophages, which is an active part of the immune system responsible for clearing foreign objects. RES organs, especially macrophages in the spleen and liver, clear a large number of particle carriers.<sup>10,11</sup> Changes in material type (lipid-based, polymeric, metallic)<sup>12</sup>, size (nanometer to micron scale)<sup>13</sup>, drug loading method (encapsulated, ionic interaction, or covalently linked)<sup>14</sup>, and surface chemistry (use of targeting ligands, charge) have been explored to alleviate RES particle clearance.<sup>15</sup> Researchers showed that the fate of intravenously injected spherical carriers is greatly affected by the particle size.<sup>16–21</sup> After eluding the clearance mechanisms of the RES, particles must navigate the dynamic blood stream to marginate to the vessel wall, interact with the correct tissue and cell type, and release the payload for maximal therapeutic effect. These processes present a complex series of hurdles unique to particulate drug carriers that remain weakly understood.

In the design of targeted carriers, it is imperative to engineer for the entire biological journey, from injection to the intended site of delivery, to achieve maximal targeting efficacy. The particles must successfully evade immune capture, distribute to the targeted organ, localize to the endothelial layer of a blood vessel, be taken up by cells of interest, and release drugs on an appropriate time scale for the specified disease. Given this complex series of barriers, further understanding of targeted particle delivery systems is required before becoming commonplace in the clinic. Control of particle geometry holds great promise in improving the efficacy of spherical targeted particulate carriers.<sup>22–24</sup> To date, most studies use spherical particle therapeutics, due to the ease of fabricating such particles. With the recent advent of new particle fabrication techniques, researchers are increasingly able to generate particle geometries similar to those found in nature, mimicking the physical properties of red blood cells (RBCs), pollen spores, and bacteria, to name a few.<sup>25–32</sup> To this end, shape has emerged as a critical component of targeted carrier design and has the potential to enhance the performance of targeted carriers in a wide range of diseases.

While much research has focused on the effect of particle shape in drug delivery, there is a lack of conclusive evidence of which particle geometries are ideal – largely because particle shape affects many biological and interfacial phenomena (margination, cell adhesion, cellular uptake, phagocytosis, etc.) in different ways. Further, the outcome of an injected carrier is not determined solely by shape, but is confounded by other parameters including size, density, material type, and surface characteristics. This review covers the findings to date concerning particle shape effects on the biological processes relevant to drug delivery, including interaction with the RES, biodistribution, margination, intracellular uptake/trafficking, and drug release.

## Effect of Particle Shape on Clearance at the Cellular, Tissue and Organ Level

The immune system is highly efficient at identifying and removing foreign matter, thus, particulate drug carriers must be carefully engineered to evade the variety of physiological clearance mechanisms. All particles, no matter the size, are subject to immune clearance; physical barriers in the kidney, lungs, liver, and spleen offer geometric restrictions to particles, while phagocytic cells such as macrophages continually engulf particles. Recent research has shown that RES clearance is not only dependent on particle size, but is also dependent on other geometric features such as surface curvature, axis lengths, and aspect ratio (AR). These interactions on the cellular and tissue level have a global impact on the fate of the carrier in an *in vivo* model. This section discusses recent findings of how particle shape affects interactions with and clearance by the RES system. These studies, ranging from cellular interactions to tissue accumulation, produce particle shape guidelines to evade immune clearance and extend particle blood circulation time *in vivo*.

### Macrophage Uptake and Frustration

Macrophages clear entities such as dead or damaged cells, bacteria, or pathogens, ranging in size from 1  $\mu\text{m}$  to 10  $\mu\text{m}$ , from the blood stream via phagocytosis. Proposed drug delivery systems on the micron and sub-micron scale have typically had spherical geometry, which macrophages readily phagocytose. Recent research, mostly conducted with murine macrophages, has clarified that particle geometry is as important as particle size in determining macrophage uptake efficiency and speed.

Researchers utilized a murine cell line to investigate macrophage attachment and passive uptake of non-targeted particles *in vitro*. Devarajan *et al.* found that 200–400 nm spherical lipomer particles were more readily taken up by macrophages as compared to irregularly shaped lipomers, which they speculated was due to incomplete actin structure formation during macrophage wrapping of different particle features.<sup>17</sup> Lu *et al.* fabricated spheres, rods, and needles of CdTe-cysteine composites and showed decreasing macrophage uptake with increasing particle AR.<sup>33</sup> Doshi and Mitragotri demonstrated, as shown in Fig. 1, that macrophage attachment is dependent on shape and size of the target object; specifically, macrophages attached most efficiently to polystyrene (PS) particles with the longest dimension in the size range of the most abundant bacteria found in nature (2–3  $\mu\text{m}$ ).

Macrophage membrane ruffles may play an important role in the attachment and the determination of how particles orient themselves relative to the macrophage.<sup>21</sup> Champion and Mitragotri engineered polymeric particles to evade macrophage uptake and found that particles with ARs above 20, and major axes of 9  $\mu\text{m}$  and 27  $\mu\text{m}$  respectively, showed negligible phagocytosis as compared to spherical particles, likely due to the extremely low curvature along the majority of the particle.<sup>34</sup> Lin *et al.* noted the lack of importance of shape for phagocytosis below 70 nm when comparing spherical and hexagonal major axis length, but demonstrated the increasing importance of shape at a larger axis length of 120 nm.<sup>35</sup> Arinda *et al.* demonstrated a longer circulation time for gold nanorods of AR 4.5 as compared to gold nanospheres. They explained this by showing that *in vitro* murine macrophages uptake gold nanospheres four times more efficiently than nanorods.<sup>36</sup> Sharma proved that macrophage attachment and uptake of PS particles are independently affected by shape; macrophages phagocytosed oblate ellipsoids most efficiently, but prolate ellipsoids showed the most cellular attachment.<sup>37</sup> The overwhelming trend shows by increasing particle AR, especially on the micron scale, the efficiency of phagocytosis by macrophages in a murine macrophage line decreases significantly.

While the effect of shape on phagocytosis is clear, the mechanism by which macrophages sense the size and shape of their targets is of interest. Champion and Mitragotri defined a dimensionless parameter,  $\Omega$ , which incorporates both the curvature of the particle and the attachment point of a macrophage, as shown in Fig. 2A. When  $\Omega$  exceeded  $45^\circ$ , with decreasing surface curvature, the macrophages did not internalize the PS particle of interest and the membranes simply spread; the paper defined this as frustrated phagocytosis. Phagocytosis became less likely with smaller  $\Omega$ s as volume increased, as shown by Fig. 2C.<sup>38</sup>

This work highlights how macrophages use local surface curvature to extrapolate the size of particles; a low local curvature gives the impression of an infinitely large object. Geng *et al.* found that macrophages failed to uptake polymeric filomicelles longer than 3  $\mu\text{m}$  *in vivo*, reinforcing that particles with high ARs and very low local curvatures are not efficiently phagocytosed. Once the filomicelles degraded into smaller pieces they were readily uptaken by macrophages.<sup>39</sup> Schinwald *et al.* tested the phagocytosis limits of alveolar macrophages using silver nanowires of constant diameter and increasing lengths. They found that nanowires up to 10  $\mu\text{m}$  in length were phagocytosed completely, but those 14  $\mu\text{m}$  and larger induced frustrated phagocytosis and were shared between adjacent macrophages.<sup>40</sup> Dasgupta *et al.* utilized simulations to produce phase diagrams that predict completeness of wrapping, based off of cell membrane tension and particle-cell interaction strength, as shown in Fig. 3. Incompletely wrapped particles fell into the frustrated phagocytosis category.<sup>41</sup> Theoretical and experimental results agree that frustrated phagocytosis arises at the two extremes of curvature of high AR particles, and also depends heavily on total particle volume.

As we previously alluded to, only a few *in vitro* experiments have used human macrophages to investigate phagocytosis. In one work, Bartneck *et al.* found that neutral gold nanospheres were entrapped at a much higher level than neutral gold nanorods, which is in line with the bulk of the findings with murine macrophages. However, particle shape did not appear to



inability of nanoworms to navigate the splenic filter and resulting discrepancy in observed trends. Arnida found that while both PEGylated gold nanospheres and nanorods accumulated significantly in the spleen, the nanorods showed lesser accumulation prior to a week, thus allowed longer circulation time in vivo.<sup>36</sup> Lin *et al.* found that in mice, biocompatible hexagonal NPs accumulated twice as efficiently in tumors compared to spherical NPs by evading spleen and lung filtration.<sup>35</sup> In general, researchers have found the minor axis of particles more accurately predicts spleen entrapment, thus confirming that the alignment of particles in the direction of flow allows avoidance of spleen filtration.

The characteristics of sinusoidal spleen filtration varies across animals, as the type and size cutoff of spleen filtration varies.<sup>47</sup> Akiyama *et al.* found that gold nanorods with constant volume and ARs 1.7 and 5.0 distributed differently in the mouse spleen. Nanorods with a 50 nm major axis accumulated slightly more in the spleen as compared to the rods with a 17 nm major axis, showing that splenic entrapment in mice could be dependent on AR even below the human filtration cutoff.<sup>49</sup> Nevertheless, one must keep in mind that animals do not always directly scale with the human body; the murine spleen is known to have very small venous sinuses and a different distribution of immunoactive cell types.<sup>46</sup> Also, there is evidence that size alone does not determine particulate fate in splenic filtration; tailoring the size, shape, and modulus of hydrogel particles to mimic RBCs in mice minimized filtration by the spleen and lungs.<sup>16</sup>

Splenic filtration and clearance is a complex mechanism that relies on a combination of particle shape, size, hydrophilicity, and modulus to entrap foreign or damaged entities. If the target of the drug delivery system is the spleen, the innate filtration mechanism can be exploited to increase accumulation. Spleen pore size historically limited spherical particles larger than 500 nm from efficient targeted delivery, but non-spherical geometries have opened the door to using particles with larger volumes but with a minor axis smaller than the pore size of the spleen.

### Kidney Filtration

The kidney's glomerular filtration relies on the diffusion of small compounds through the fenestrated capillary endothelium and across the subsequent podocyte filtration slits. The kidney freely filters particles and compounds with a radius less than 6 nm. Most drug delivery particle systems are too large for kidney filtration.<sup>50</sup> Particles would have to align with the endothelial pores for filtration, an unlikely occurrence given the simulated flow dynamics of non-spherical particles; non-spherical particles align with the long dimension parallel to the direction of flow.<sup>39</sup> Following this, Park *et al.* found that iron oxide nanoworms accumulated significantly less in the kidney compared to spheres; their length of 50 nm exceeded the filtration limit.<sup>48</sup> Akiyama *et al.* logically found no difference in kidney accumulation of constant volume gold nanorods with ARs 1.7 and 5.0 and major axes of 10.6 nm and 49.6 nm in tumor bearing mice.<sup>49</sup> Overall, kidney clearance can be diminished or eliminated if one axis of the particle is larger than 6 nm, irrespective of the specific shape. This is in stark contrast to small molecule drugs, which are often limited by renal clearance and toxicity.<sup>51</sup>

## Liver Entrapment and Digestion

The liver is considered an organ of the digestive system but also plays a large role in RES responses. In the context of the RES, the liver is comprised of hepatocytes that serve to metabolize foreign or toxic substances, as well as liver-specific macrophages called Kupffer cells. The blood flow splits into discontinuous sinusoids lined with fenestrated endothelium with gaps up to 150 nm. Hepatocytes project into the blood flow, forming a layer behind the endothelium and phagocytic Kupffer cells.<sup>52</sup> Kupffer cells account for 80–90% of fixed macrophages in the entire body and use foreign surface protein patterns to identify foreign entities, thus, the liver is a highly immunoactive organ.<sup>53</sup>

Hepatocytes and Kupffer cells both metabolize foreign or toxic materials. The size of particles entrapped by the liver is controlled by both the size of capillary fenestrations and the Kupffer cells. Akiyama *et al.* found no difference in liver accumulation of constant volume gold nanorods with ARs 1.7 and 5.0 and major axes of 10.6 nm and 49.6 nm in tumor bearing mice.<sup>49</sup> This is logical as the liver capillary fenestrations are larger than both particle types. Devarajan *et al.* reported that spherical lipomers with diameters ranging from 350 nm to 450 nm accumulated in the liver, whereas the irregularly shaped lipomers accumulated in the spleen. Overall, particles smaller than the fenestrated capillaries successfully pass through given successful Kupffer cell evasion.

## Effect of Shape on Biodistribution

The previous sections described how particles interact biologically on a cellular and tissue level. Subsequently, these interactions will dictate the overall fate, or biodistribution, of a particle in an animal. Particles will continue to pass through the various filtration systems and RES mechanisms and ultimately distribute to tissues throughout the body. One challenge with the implementation of injectable micro/nanocarriers is in understanding, and more importantly, controlling the fate of the carrier system. Typically, particulate drug carriers large enough to avoid kidney clearance accumulate in the organs of the RES, with the majority of the dose removed from circulation in minutes to hours. Biodistribution can be altered or improved by modifying the particle surfaces with various ligands;<sup>54</sup> using elongated particles may enhance the efficacy of these ligands. Researchers experimentally showed that by altering shape, particles remained in circulation longer, shifting the biodistribution from their spherical counterparts to direct accumulation to specific tissues or organs.

Within the past several years, multiple studies using lipid, polymer, or metal-based carriers have shown that shape can affect the circulation and biodistribution of injectable micro or nanoscale carriers, resulting in improved therapeutic outcomes *in vivo*. Decuzzi *et al.* investigated the murine biodistribution of silica micro and nanoparticles of varied shapes (spherical, cylindrical, discoidal, and quasi-hemispherical) and sizes (0.7–3  $\mu\text{m}$  of equivalent spherical diameter, or ESD).<sup>55</sup> They found that discoidal particles accumulated less in the liver, but more in the lung and spleen, as compared to spherical, quasi-hemispherical, and cylindrical particles. The lesser accumulation of discoids in the liver was attributed to the ability of elongated particles to evade phagocytosis by Kupffer cells, while the less elongated particles were phagocytosed more efficiently. Researchers have investigated

Author Manuscript

Author Manuscript

Author Manuscript

polymer-lipid NPs for passive splenotropic drug delivery and found that irregular, non-spherical particles showed a 4 to 12 time increase in the spleen to liver accumulation ratio as compared to spherical particles.<sup>17</sup> Accumulation of rods was mainly found in the liver, lung, and spleen; the shorter rods were found at higher levels in the liver relative to long rods, and the longer rods accumulated more in the spleen – results which are potentially related to splenic pore filtration size and Kupffer cell phagocytosis. Arnida *et al.* reported that gold nanorods had a longer circulation time, decreased liver accumulation, and increased tumor accumulation compared to gold nanospheres in tumor bearing mice.<sup>36</sup> Similarly, Park *et al.* showed that iron oxide nanoworms remained in circulation longer and passively or actively targeted tumors in mice better than iron oxide nanospheres.<sup>48,56</sup> Muro *et al.* investigated the circulation time of spheres and elliptical disks coated with a targeting ligand to intercellular adhesion molecule-1 (ICAM-1), and found that targeted elliptical disks ( $0.1 \mu\text{m} \times 1 \mu\text{m} \times 3 \mu\text{m}$ ) were able to remain in circulation after 1 min and 30 mins at higher concentrations than microspheres ranging in size from 0.1–10  $\mu\text{m}$  in diameter.<sup>57</sup> A recent study by Zhang *et al.* shows that loaded polymer nanodisks delivered doxorubicin (DOX) to the tumors of mice at nearly ten-fold the level of equivalent solutions of DOX, however, the nanodisks were not compared to nanospheres loaded with DOX. Thus, it is not clear how much of this particular effect was specifically due to particle shape.<sup>58</sup> By elongating particles to reduce local surface curvature, phagocytosis becomes frustrated, resulting in lower liver accumulation, which is potentially useful for application in cancer therapeutics shown to cause hepatotoxicity.<sup>59</sup>

Author Manuscript

Author Manuscript

Though many of the aforementioned studies shed valuable insight into the effect of shape on the biodistribution of particles, most show rapid immune clearance due to the particle composition and rapid protein opsonization. Poly (ethylene glycol) (PEG) is a hydrophilic polymer that has been reviewed and used extensively to slow plasma protein opsonization when present on particle surfaces, thereby allowing particles to evade immune recognition.<sup>60</sup> The efficiency of PEG as a coating for reducing opsonization is highly dependent on the particle surface PEG concentration; low concentrations do not show efficient repulsion of plasma proteins whereas high concentrations, in the brush regime, allow for the most efficient immune evasion. Due to steric reasons, the achievable surface density of PEG decreases with increasing PEG molecular weight and increasing particle radius (i.e. decreasing surface curvature).<sup>61</sup> For complex shapes, the local curvature changes widely across the surface, thus creating a non-uniform coating of PEG.

In general, PEGylated particles show longer circulation times. Geng *et al.* showed that filamentous micelles (or “filomicelles”) with hydrophobic cores and hydrophilic PEG shells had longer circulation times in mice compared to similarly composed spherical micelles on the micron to submicron scale.

Author Manuscript

Interestingly, these filomicelles persisted in circulation up to a week after injection, even with major axis lengths over 8  $\mu\text{m}$ , while their spherical counterparts were cleared within a day or two.<sup>39</sup> A subsequent study by the same lab showed delivering the cancer drug paclitaxel via filomicelles to tumor bearing mice produced an increased local, tolerable drug dosage compared to spherical micelles, which resulted in a more effective tumor treatment (Fig. 4).<sup>62</sup> This effect is potentially due to a combination of (a) fragmenting by non-



phagocytic cells, leaving smaller filomicelles in circulation and (b) the inefficient uptake of elongated particles by phagocytes shown *in vitro*.<sup>38,63</sup>

Researchers use PEGylated gold nanorods for plasmonic photothermal therapy<sup>64</sup> and a detailed study showed that gold nanorods with ARs of 1.7 to 5.0 and diameters of 10 nm to 50 nm all showed similar biodistributions. Therefore, researchers concluded that gold nanorod biodistribution is controlled mostly by PEG density, surface characteristics, and zeta potential, not AR.<sup>49</sup> Perry *et al.* showed that 80 nm × 80 nm × 320 nm nanodisks with both low density mushroom PEG and high density brush PEG showed diminished macrophage uptake and improved circulation time over non-PEGylated nanodisks. Particles with brush conformation showed better immune evasion than mushroom conformation.<sup>54</sup> Huang *et al.* studied the biodistribution and clearance of rod-shaped mesoporous silica NPs, both bare and PEGylated, with two different ARs (1.5 and 5) and lengths (185 nm and 720 nm, respectively) in mice. They found that RES capture and clearance was slower for the rods with a higher AR and slower for PEGylated particles than bare particles; the particles with the highest AR and PEG showed the longest circulation time.<sup>65</sup> Park and coworkers used targeted, iron oxide nanoworms and showed that those with a surface PEG linker were taken up less into cells, but speculate that they will show longer circulation time due to stealthness.<sup>48</sup> Researchers showed that ellipsoidal polyaspartamide polymersomes with the highest concentration of both a PEG linker and adhesive terminal RGD peptide increased adhesion to endothelial cells compared to non-PEGylated and non-adhesive particles under flow conditions, but did not evaluate uptake.<sup>66</sup> Generally, PEG slows the uptake of particles but increases circulation time by evading RES clearance, thus causing a tradeoff in *in vivo* functionality.

The emergence of poly (zwitterionic) surface functionalization has attempted to address the slow uptake of PEGylated particles. Zwitterionic surface coatings offer comparable stability *in vivo* as PEG but improved and restored binding affinity and cell uptake kinetics.<sup>67</sup> However, no work has been done to show how shape changes the behavior of materials with zwitterionic surfaces.

Though the optimal particle size and shape may vary depending on the desired disease target, these studies all suggest that altering shape can be used to improve circulation time and direct biodistribution to improve therapeutic outcomes. These studies also show that PEGylation further enhance the circulation time and biodistribution of non-spherical particles; the combination of shape and surface functionalization holds great potential for maximizing the efficiency of targeted carrier systems.

## Effect of Shape on Margination

In addition to evading the numerous clearance mechanisms of the body, vascular-targeted carriers (VTCs) must navigate the dynamic environment of the blood stream in order to reach the target tissue. Whether actively targeting the endothelium via surface bound ligands or passively targeting via the EPR effect in “leaky” vasculature, the ability of an injected carrier to “marginate”, or localize and adhere to the periphery of the vessel in blood flow, is key. Margination historically described the ability of circulating leukocytes and platelets to

localize to the cell-free layer (CFL), a plasma-rich layer devoid of RBCs adjacent to the endothelium, and adhere to ECs in the presence of shear forces. Similarly, an injectable carrier ultimately meant to target the endothelium should exit the RBC core and marginate under physiological conditions. Recent studies have attempted to clarify the effect of particle shape on margination propensity.

### Margination in Simple Flows

Multiple mathematical models have predicted that under certain hydrodynamic conditions, elongated particles experience a preferential lateral drift towards the vessel wall that spherical particles do not.<sup>68–74</sup> Gavze and Shapiro developed a model which predicted lateral drift of spheroidal particles near a wall in flow, the magnitude of which increases with particle inertia.<sup>71</sup> A model by Lee *et al.* showed that the presence/magnitude of this lateral drift depends on the particle Stokes number, which is a ratio of the inertial and viscous forces felt by the particle.<sup>68</sup> At shear rates above  $100 \text{ s}^{-1}$ , the model showed that micron sized, non-spherical particles achieved net lateral drifts in the absence of external forces such as gravity or applied magnetic fields. This lateral drift was predicted to increase with the Stokes number, which is directly proportional to particle AR, particle ESD, and particle density.<sup>68</sup> This lateral drift allows non-spherical particles to localize to the vessel wall more efficiently than spherical counterparts.

Researchers have used flow channels with simple buffer flow to examine the margination of spherical and non-spherical particles as it pertains to microcirculation. The deposition of nonspherical particles to the wall of the microchannel was shown in some cases to be improved compared to spherical particles. Other parameters also proved important, including specific particle geometry (rod, circular disk, elliptical disk, quasi-hemisphere, etc.), particle volume, particle density, channel geometry, and shear rate.<sup>18,75,76</sup> Doshi *et al.* found that circular disks, elliptical disks, and rods with ESD on the micron scale deposited at higher levels than spheres near a bifurcation in the flow channel.<sup>76</sup> The increased adhesion compared to spheres seen for elongated particles is more pronounced with increasing particle ESD and with increasing AR, though there did not appear to be a consistent trend to suggest one particular shape is superior to others. Size, in addition to shape, is still of importance as disks and rods with  $1 \mu\text{m}$  ESD deposited at lower levels than equivalent spheres in the straight inlet region of the channel, while larger non-spherical particles consistently displayed improved adhesion compared to spheres.<sup>76</sup> Gentile *et al.* found that micron-sized discoidal and quasi-hemispherical silica particles had higher margination propensities compared to spherical silica, as the more elongated discoidal particles displayed the highest levels of margination.<sup>75</sup> A study by Toy *et al.* showed that gold nanorods displayed a higher deposition to a microchannel wall than gold nanospheres.<sup>18</sup> These results are interesting in that these particles are on the nanoscale, contradicting other works that show that as particle ESD decreases, improved margination of elongated particles relative to spheres diminishes.<sup>68,76</sup> However, it is expected that particle density, as well as size and shape, play a role in the magnitude of the lateral drift felt by particles in flow. As Lee *et al.* showed, lateral drift velocity scales proportionally with the particle Stokes number (and thus, particle density).<sup>77</sup> Therefore it is possible that the gold nanorods have a great enough density ( $\sim 19 \text{ g/cm}^3$ ) to display lateral drift producing improved margination, while the

lateral drift of less dense nanorods of the same size remains insignificant. These works demonstrate that altering particle shape can improve margination dynamics. Recently, more attention has been given to how these results translate to physiological flows; particularly those that include blood components.

### Margination in Physiological Conditions

It is well known that RBCs play a role in the margination of leukocytes and platelets, thus, it is important to determine how RBCs influence particle margination. Researchers have shown that for rigid and deformable particles the ability to marginate in the presence of blood components is highly dependent on size.<sup>7,19,78–81</sup> In general, particles with diameters on the order of microns (interestingly about the same size as a platelet) preferentially displace to the CFL in the presence of RBCs, while smaller particles do not experience this enhanced localization.<sup>19,78–81</sup> Recent work in our lab has investigated how particle shape affects margination due to interaction with RBCs in flow. Thompson *et al.* observed improved adhesion of microrods to a human umbilical cord EC (HUVEC)-lined wall in a microchannel when compared to equivalent spheres in a high shear flow of RBCs, provided the particle AR and volume were of sufficient magnitude.<sup>82</sup> However, when localization to the CFL in RBC flows was imaged via confocal microscopy, no difference between the localization of rods and equivalent volume spheres was observed, suggesting the observed improved margination of microrods in flow over microspheres is due mainly to improved adhesion conditions. Our group also recently tested adhesion between rods and spheres to the aortae of Apolipoprotein E double knock out mice, a common murine model of atherosclerosis. We found that microrods bound at much higher levels to the aorta than microspheres (Fig. 5), while nanorods and nanospheres both displayed minimal adhesion, as was seen in *in vitro* flow chamber studies.<sup>83</sup>

A recent mathematical model aligns well with these experimental results. The study presented both 2-D and 3-D models of RBC/rigid particle mixtures in confined flows, much like the aforementioned experimental setup. The model, shown in Fig. 6, suggested that while ellipsoidal particles will display equal or lesser margination compared to equivalent spheres, the more favorable adhesion characteristics of ellipsoids, as they present more targeting ligands per particle volume and can initiate contact further from the endothelium, could result in higher adhesion levels than that of spheres.<sup>84</sup>

Another multi-scale model that combined both localization and adhesion dynamics predicted that in low shear blood ( $2\text{--}10\text{ s}^{-1}$ ) flow, nanorods have a higher binding probability than nanospheres.<sup>85</sup> However, this higher binding probability of nanorods was not seen *in vitro* with blood flow at higher shear rates more likely to be encountered in the bloodstream.<sup>82</sup> This recent work has demonstrated the importance of including physiological components, such as RBCs, in mathematical and experimental models.

### Margination Implications for Biodistribution and Targeting Specificity

Other recent studies investigated how shape affects the biodistribution of particles coated with ligands for active targeting. Kolhar *et al.* investigated the biodistribution of spherical (200 nm diameter) and prolate ellipsoidal (AR = 4, 500 nm major axis) PS particles targeted

to ICAM-1, an EC receptor associated with inflammation.<sup>86</sup> By coating particles with the targeting ligand instead of a non-specific IgG, accumulation in the lungs of mice was increased for both spheres and rods; however, Fig. 7 (A–D) shows the effect was more pronounced for rods likely because the rod shape is favorable for adhesion by targeting ligands. Nanorods coated with a ligand that binds the transferrin (TfR) receptor for targeting of the brain endothelium also accumulated at higher levels in the target tissue of the brain (and other major organs) compared to TfR-targeted nanospheres.<sup>86</sup>

Muro *et al.* investigated the biodistribution and targeting efficacy of spheres and elliptical disks targeted to ICAM-1, and found that elliptical disks had a better targeting specificity to the lung vasculature compared to spherical particles (Fig. 8).<sup>57</sup> Overall, elongated, streamlined particles have more favorable adhesive characteristics as compared to spherical particles for a number of reasons. The smaller cross-sectional area normal to flow reduces the shear removal force imparted by blood flow that would remove a particle already adhered to the endothelial wall. Elongated particles interact more efficiently with their target site in the presence of shear forces compared to spherical or non-elongated particles.<sup>76,82,83,87</sup> Particle elongation also allows the presentation and interaction of more surface-conjugated targeting moieties with the target site compared to equivalent spherical particles.<sup>87</sup> This improved adhesion is more pronounced for microparticles compared to NPs, for which incremental improvement in drag reduction or ligand presentation may be negligible due to the smaller overall particle size.

It is critical that researchers consider potential unintended consequences of increased adhesion propensity of elongated particles; specifically, elongated particles may present higher accumulation in non-targeted organs. This was observed in a recent study in our lab, where microrods and microspheres were used to target atherosclerotic plaque via inflammatory receptors on the ECs. While elongated microparticles targeted plaques better than spherical counterparts, they also exhibited greater accumulation in the lungs, seemingly due to molecular interaction with inflammatory receptors on lung ECs.<sup>83</sup> The choice of highly site-specific targeting moieties becomes increasingly important for non-spherical particles, particularly if the target receptor has a basal level of expression on healthy ECs.

As it stands, more mathematical and experimental works need to be done to fully elucidate the effect that particle shape has on margination, particularly in the presence of blood components and more complex conditions representative of human physiology. Ultimately the effect of shape on margination will likely be coupled to multiple particle parameters including size, flexibility, and density; thus the design of VTCs must consider local hemodynamics near the desired target.

## Influence of Particle Shape on Cell Uptake

Following navigation through organ-level barriers, avoidance of phagocytes, and margination to the endothelium, targeted particle carriers must then reach their target cell. Often, the site of action for the drug cargo requires travel outside of the vasculature. Thus, cellular uptake is another crucial hurdle to be addressed and studied in the drug delivery process. Non-targeted particles must passively travel across or between cell membranes,

whereas targeted particles capitalize on receptor-mediated internalization. In applications focused on vascular imaging, vessel disruption in cancer, or gene delivery for regulation of specific EC-expressed proteins, drug carriers need to only marginate, bind to the vascular wall, and be internalized (endocytosed) by ECs. For drugs that must reach a location beyond the ECs, carriers need to transcytose through the ECs or must pass through cell-cell junctions. Most recent works focus on particle internalization; therefore, overarching conclusions may not be made about transcytosis.

Works to date that address cellular internalization of carriers focus on spherical, cylindrical, discoidal, or rod-shaped particles. There is consensus in the literature that particle shape affects particle uptake rate, uptake mechanism, and total accumulation; however, the exact way in which shape affects these results is still under debate. Conflicting results have been reported, most likely owing to the confounding variables of particle size, surface chemistry, surface charge, flexibility, and cell type. A range of physiochemical properties works together to influence cellular uptake patterns, and will be discussed along with the trends in particle shape effects on cell uptake. Much of the experimental work to date investigates cellular uptake by a specific cell line under static conditions with the goal of producing uptake kinetics and final overall uptake. These pioneer studies clearly determine that uptake mechanism and internalization kinetics are dependent on particle shape. As the field progresses, research continues to shed light on the underlying complexity of how particle shape affects cellular and tissue uptake.

### Theoretical Wrapping of Particles by Elastic Lipid Bilayers

The cell membrane, a fluid lipid bilayer, does not engulf all entities presented at its surface. Rather, a complex interplay between the adhesion energy gain (contributed by the particle-bilayer interaction) and bending energy loss determines the kinetics and ultimate fate of wrapping. Passive translocation, i.e. ATP-independent endocytosis, of ultra-small NPs (0.1–2 nm) across a lipid bilayer occurs without active membrane wrapping. However, the process requires a positive energetic driving force, such as the interaction between ligand and receptor, and the internalization rate and result depends on the orientation of contact, total contact area, and total volume of the particles.<sup>88</sup> Simulations of passive, i.e. non-receptor limited, endocytosis revealed that larger, spherical NPs, up to 14.3 nm in diameter, promote spontaneous internalization. Interestingly, spherocylinder and cylinder particles change orientation during endocytosis to maximize the particle ligand-cell receptor interactions and to minimize bending energy expended (Fig. 9A). No internalization fate difference was found between cylinders of lengths 8 nm or 16 nm and an 8 nm diameter sphere. Overall, cylinders were never fully internalized, no matter the ligand-receptor binding strength, due to the high local curvature on the edges, as shown in Fig. 9B.<sup>89</sup>

Decuzzi and Ferrari utilized a continuum energetic approach to simulate the effect of particle shape and size on receptor-mediated endocytosis, taking into account both bending of the membrane and internal cytoskeleton. They noted that as the curvature of a particle changed incrementally, i.e. non-continuously, the speed factor of the wrapping changed incrementally as well. Upper and lower critical ARs were defined; particles with ARs above the upper critical AR produced only partial wrapping, and particles with ARs below the lower critical

AR never induced wrapping. As shown in Table 1, the critical ARs are dependent on volume, for example, for particles volume-matched to spheres with diameter of 50 nm, the critical ARs are 0.84 to 1.19, whereas for particles volume-matched with 500 nm spheres 0.18 to 5.54 are the critical ARs.

The same work determined that the internalization of elliptical cylindrical particles is highly dependent on the overall volume and the AR of the particles.<sup>90</sup> Bahrami identified two distinct stages of cellular wrapping, spreading and internalization, which are separated by a crucial energy barrier. Specifically, ellipsoidal particles with higher ARs present the highest energy barrier for internalization, and the ellipsoidal wrapping proceeds via orientation shift from parallel to more perpendicular.<sup>91</sup> Dasgupta *et al.* theoretically confirmed the prediction of particle reorientation during the wrapping process due to non-uniform curvature in rods. Additionally, they produced general phase diagrams that determined when shallow, deep, or complete wrapping would occur for shapes such as cylinders or cubes, depending on the particle-cell adhesion strength and membrane tension. From this, they concluded that size and AR were not enough to determine the endocytic state, but rather the extrema of the local curvature determines the final wrapping state of the particle (Fig. 3).<sup>41</sup> Finally, Kolhar *et al.* noted that the entropic loss required to uptake non-targeted particles increases with particle AR, but that for particles targeted with antibodies the adhesion interaction can overcome these entropic losses.<sup>86</sup>

These crucial simulations highlight the complexity of elastic membrane wrapping, stressing the importance of membrane rigidity, local geometric properties, targeting ligand density, and ligand-receptor interaction strength. These simulations elucidate the issue of a highly curved feature on a particle that might interact with the cell membrane—it will highly discourage membrane wrapping and cell uptake. Further simulations that incorporate the effects of shear from a hypothetical blood vessel would add another level of complexity to help predict reality of *in vivo* particle uptake.

### Experimental Cell Uptake

A myriad of *in vitro* studies have attempted to identify the effect of particle shape on cellular internalization patterns. Before the development of fabrication methods that delivered more control over the shape and monodispersity, such as PRINT<sup>92</sup>, changing particle shape was synonymous with varying the AR. Now a myriad of particle shapes beyond ones within the ellipsoidal/spheroidal family can be achieved with the rapid development of fabrication methods that produce more complex, well-controlled shapes.<sup>25–32</sup> As these different particle shapes are fabricated and evaluated, experimental cellular internalization results continue to conflict one another, likely due to confounding variables such as cell type, particle size, and surface properties.

Gold NPs showed early potential as a drug or imaging agent carrier. Chithrani *et al.* probed the dimensional limit of gold NPs and showed the rate and cumulative non-specific uptake of gold nanorods decreased in HeLa cells with particle AR increase from 1 to 5.<sup>20</sup> Targeted, transferrin-coated gold NPs were evaluated in alternative cell lines, and the results confirmed the diminishing uptake of gold rods with increasing AR in all cell types. Gold nanorods were internalized 5–7 times less than spheres of the same volume, depending on the cell

line, and the authors concluded that the wrapping time controlled the uptake kinetics.<sup>93</sup> For non-targeted, gold particles with features between 10 nm and 100 nm, spherical particles delivered the most efficient and largest uptake *in vitro* as compared to rods.

Gratton *et al.* investigated internalization of non-targeted PEG cubes and cylinders of varying size and AR. HeLa cells internalized cylinders with the highest AR (150 nm × 450 nm) the fastest and to the greatest extent.<sup>94</sup> On the contrary, Muro reported four times slower uptake of PS anti-ICAM ellipsoidal disks (0.1 μm × 1 μm × 3 μm) as compared to 5 μm spheres.<sup>57</sup> Different size scales (nm vs. μm) may explain these contradictory results, as radius of curvature was shown important with macrophages. Smaller particles provide a smaller area of extremely low curvature, which is difficult for particles to wrap with increasing volume. Yoo *et al.* found PS spheres (1 μm) and elliptical disks (0.2 μm × 0.7 μm × 3.5 μm) accumulated into ECs *in vitro* in similar amounts after long times, but that 1.8 μm poly(lactic-co-glycolic acid) (PLGA) spheres were internalized more quickly than ESD PLGA elliptical disks with an AR of 5. The initially faster uptake rate of spheres was eventually equilibrated and after 4 hours the total internalization of the spheres and disks was equivalent.<sup>95</sup> Both the rate and overall internalization of hollow poly(methacrylic acid) capsules internalized by HeLa cells decreased with increasing AR.<sup>96</sup> Agarwal *et al.* probed the internalization of PEG disks and rods in 4 different cell lines (Fig. 10 A–F).

While the trends are cell specific, the nanodisks were internalized the most efficiently, and overall, larger particles were internalized more than smaller. Additionally, cells internalized larger disks and rods more effectively than spheres, which is a trend reversal compared to spheres that typically display reduced internalization efficiency as their size increases. The authors identified sedimentation to the cell layer, membrane deformation required, and adhesion forces resulting from contact area as important factors for static *in vitro* uptake. The more efficient internalization of larger rods and disks was attributed to the larger surface area in contact with the cells, and thus, more multivalent interactions for particle uptake.<sup>97</sup>

Silica, a non-polymeric biomaterial, has gained attention for its biocompatibility and potential for drug delivery and imaging applications. Huang *et al.* used human melanoma cells to demonstrate that mesoporous silica NPs with larger ARs, up to 4, were taken up in larger amounts and have faster uptake kinetics.<sup>98</sup> However, Meng *et al.* identified an ideal AR of 2.1–2.5 for the maximal uptake and fastest internalization kinetics of mesoporous silica NPs in HeLa cells.<sup>99</sup> This disparity in ideal AR might be attributable to cell type and difference in total particle volume. Human epithelial cells initially internalized silica spheres, cylinders, and worms at different rates due to differing uptake mechanisms, but equilibrated to a level independent of geometry.<sup>100</sup> She *et al.* fabricated hollow silica capsules to mimic RBCs and found that hollow silica spheres are internalized 1.6 times more efficiently than disks by smooth muscle cells.<sup>101</sup> Hamster ovary cells found rigid silicon nanowires, functionalized with folate, difficult to internalize if longer than 5 μm; the rigidity inhibited any additional adhesive interactions.<sup>102</sup>

Clearly, shape plays a large role in determining the total and kinetics of cellular uptake. The range of experimental cell uptake results spanning differences in particle matrix, geometry, volume, surface chemistry, along with differences in cell line and dosing conditions makes it

difficult to tease out true, overarching shape conclusions. Although experiments conducted in static shed valuable insight into cellular uptake trends *in vitro*, the experimental set up is not fully representative of dynamic blood flow conditions that particle systems encounter *in vivo*. Thus, it remains important to study cell uptake under hemodynamic forces in blood flow.

### Effect of Particle Shape on Different Cellular Uptake Mechanisms

Internalization can result in specific cellular signaling depending on the exact uptake mechanism.<sup>103</sup> Mammalian cells utilize endocytosis, the energy-dependent uptake mechanism, to engulf and internalize extracellular entities such as viruses, proteins, and synthetic particles. There are four main endocytic pathways identified to date: (1) macropinocytosis, (2) clathrin-mediated endocytosis, (3) caveolae mediated, and (4) clathrin- and caveolae-independent endocytosis, although it is speculated that more mechanisms exist.<sup>57</sup>

The mechanism of uptake is controlled by size, shape, surface chemistry, and possibly material characteristics. Identification of the specific uptake mechanism is determined through biochemical silencing of each uptake mechanism in order to isolate the mechanism that controls uptake kinetics. Gratton *et al.* found that in HeLa cells, 200 nm AR 1 and 150 nm AR 3 cylinders utilized clathrin-mediated, caveolae-mediated, and clathrin and caveolae independent uptake mechanisms. Though both type of cylinders used all three internalization mechanisms, the higher AR cylinders utilized all pathways to a larger extent, thus producing the fastest uptake rate.<sup>94</sup> Muro *et al.* recently described cell adhesion molecule (CAM)-mediated endocytosis, a condition independent of the four mechanisms listed above, where CAM receptors cluster, resulting in a unique internalization pathway. The researchers found that disks aligned with actin stress fibers slowly, thus creating initially slower uptake than spheres, which equilibrated with time. Additionally, the most potent actin-depolymerizing agent inhibited uptake of spheres up to 5  $\mu\text{m}$  and elliptical disks (0.1  $\mu\text{m} \times 1 \mu\text{m} \times 3 \mu\text{m}$ ), thus implying that all particles examined utilized an actin-dependent, non-classical, endocytic mechanism that allows for much larger particle uptake.<sup>57</sup> Agarwal *et al.* found cellular uptake mechanisms were both cell type and particle shape dependent. All else constant, the researchers concluded that shape variations induced differing efficiencies for each possible uptake mechanism.<sup>97</sup> Huang *et al.* determined that non-specific but highly efficient clathrin-mediated endocytosis facilitated the uptake of mesoporous silica nanorods into human melanoma cells.<sup>98</sup> In contrast, Meng *et al.* found mesoporous silica nanoparticle uptake mediated by GTPase-dependent macropinocytosis, which includes actin polymerization, filopodia formation, and activation of GTP-binding proteins that optimally uptakes intermediary AR rods.<sup>99</sup> Herd *et al.* investigated uptake of silica NPs and found shape dependent uptake mechanisms in human epithelial cells, specifically, invaginations associated with clathrin-mediated endocytosis for spherical particles and macropinocytosis for worm-like particles. Particles with non-spherical shapes have the capacity to present different surfaces to cells, thus allowing them to initiate and exploit multiple internalization mechanisms.<sup>100</sup>



Researchers historically defined size limitations of each uptake mechanism by observing spherical particle uptake cutoffs.<sup>104,105</sup> Recent work challenged these boundaries and showed that by altering shape, a particle of much larger volume than expected is internalized by a specific uptake pathway.<sup>94</sup>

### Extravasation and Tissue Penetration

Particle delivery and localization to tissue beyond vasculature is a critical obstacle in many drug delivery applications, including cancer therapy, brain disease treatment, muscular syndromes, and many more. Targeting efficiency of carriers targeted to tumor cells is wiped out if those particles never escape vasculature and reach the target. Thus, researchers must decide whether to target tumor ECs for transcytosis into tumors or to target cancerous cells by taking advantage of the EPR effect. Particles must extravasate in order to reach the cancerous cells; only recently have researchers studied the shape dependence of this process. Chu *et al.* studied 200 nm × 200 nm and 80 nm × 320 nm PLGA cylinders loaded with DOX in a murine tumor model and found that the smallest dimension may be the determining factor of immune clearance and entrance into the tumor; 80 nm × 320 nm cylinders resulted in slower clearance by the RES system and enhanced passive targeting by EPR in the tumor.<sup>106</sup> Chauhan *et al.* used both *in vitro* diffusion models and *in vivo* murine models to show enhanced diffusion of nanorods by an order of magnitude through collagen hydrogels and enhanced penetration into tumor tissue 4.1 times more quickly as compared to spheres. They concluded that transport across tumor-relevant pores is determined and controlled by the smallest dimension of the nanorod.<sup>107</sup> Smith *et al.* explored single wall carbon nanotubes (2 nm × 200 nm) and spherical quantum dots (d = 25 nm) with similar surface properties, surface area, and charge in three murine tumor models of extravasation. The researchers compared human brain glioblastoma (U87MG), ovarian adenocarcinoma (SKOV-3), and colon adenocarcinoma (LS174T) tumor cells via intravital microscopy in mice. The group identified three distinct trends, one for each tumor type explored: 1) only carbon nanotubes extravasated, 2) neither quantum dots nor carbon nanotubes extravasated, and 3) only the quantum dots escaped the leaky vasculature. Traditionally, spherical particles were used to determine pore sizes in a variety of tumor types, but the work of Smith *et al.* shows that spherical particles may not tell the whole story; by having one dimension pass through the smallest pores, varying shape may result in varying extravasation rates.<sup>108</sup> Most recent work shows that extravasation trends are tumor type-specific and demonstrates the need for more shape specific studies in cancer.

### Intracellular Trafficking

The intracellular fate of carriers is key, as the cargo must reach the targeted site. Once internalized, particles are released into the cytoplasm, migrate in vesicles to a location such as the nucleus, or degrade in a lysosomal compartment. Some authors have noted a lack of shape influence on intracellular particle fate.<sup>94,96,102</sup> Others agreed and further noted that volume ultimately determined particle fate; larger particles were stuck in prelysosomal compartments and smaller particles were transferred into lysosomes and degraded.<sup>57</sup> Yoo *et al.* observed a correlation between particle shape, sphere or elliptical disk, and distance from the cell nucleus at a specific time point. Namely, the spheres approached the perinuclear region 4 times faster than elliptical disks, but at equilibrium the two shapes are found in

equal proportions near the nucleus. They also note the tangential orientation of the elliptical disks to the nuclear membrane, as shown in Fig. 11.<sup>95</sup> This data leads to the conclusion that size, not shape, determines the intracellular fate of the particles, while shape may still determine spatial orientation.

Cellular internalization of non-spherical particles relies heavily on the local curvature and total volume of the particles. Simulations prove that cellular membrane tension and adhesion energy to particles is very important. Thus, the shape of particles may be tailored to shift the accumulation to the cell type of interest.

## Drug Release Profiles

Zero-order drug release kinetics has been the golden standard in drug delivery for decades.<sup>109</sup> If one can achieve sustained release at a constant rate, then a therapeutic dosage can be maintained and controlled over much longer periods of time compared to free drug administration. First and second order release kinetics still deliver an improvement over free drug, but do not achieve truly sustained release.

The release of drugs loaded physically or covalently into a biomaterial matrix depends on many factors, including drug-polymer interaction strength, diffusivity out of the particle, particle surface area to volume ratio, amount of drug loaded, and more. Shape directly affects the surface area to volume ratio, and thereby greatly changes drug release profiles. Fattahi *et al.* proposed and experimentally verified drug release profiles that scale like

$D_e M_\infty \left(\frac{A}{V}\right)^2$  by using electrojetted PLGA microspheres, microfibers, and flattened microspheres loaded with an anti-tumor agent (Fig. 12).  $M_\infty$  represents the drug loading

capacity,  $D_e$  represents diffusivity of a drug within a microcapsule, and  $\frac{A}{V}$  represents the geometry.<sup>110</sup> Yu *et al.* reported 96 hours of zero order drug release kinetics from cellulose acetate nanofibers loaded with ketoprofen. This time range represented a linear release of over 90% of the drug payload.<sup>111</sup> While they cited diffusion as the release mechanism, they did not provide any parameters used in the Fattahi findings, so it is not possible to verify their results. Similarly, Heslinga *et al.* reported that the release profile of BSA from PLGA rods can be fitted with a diffusion controlled release model for a cylinder.<sup>112</sup> Results have shown that maintaining a constant surface area to volume ratio with dissolution of particles delivers the most controlled and sustained release; this can be achieved using a variety of different shapes.

## Conclusion and Outlook

The work presented in this review proves that particle geometry is a critical parameter that controls the fate of drug delivery carriers. Particle shape is challenging to define and control from a fabrication standpoint and provides an incredible degree of design freedom, resulting in rather limited exploration of the available parameter space to date. Despite these challenges, a few trends have emerged regarding the role of particle geometry in biodistribution, immune interactions, margination, cellular uptake, and drug release. Ultimately, it will be imperative to identify optimal geometries for each of these steps, with

the eventual goal to engineer particles for a systemic approach; if changing shape improves margination but diminishes particle uptake in target cells, the trade-off is not beneficial overall.

In our review, we found evidence to support the role of particle geometry in mitigating interactions with the RES immune system. Overall, increasing particle AR was found to decrease macrophage phagocytosis efficiency, due to changes of local curvature, which promoted cellular frustration. In general, higher AR particles were found to increase circulation time by avoiding splenic filtration and liver sequestration when compared to spherical analogs, although this was dependent on the overall physical dimensions, particle matrix, and flexibility. Non-spherical particles were also shown to positively influence margination, with disks and rods improving migration to endothelial walls, although this effect was restricted to micron-sized particles under physiological blood flow conditions. Additionally, both drug release and active targeting through ligand-cell interactions were directly related to surface area, which depends on particle shape. Finally, cellular internalization rates and cellular mechanisms were shown to be loosely dependent on particle geometry, but were confounded by differences in exact particle geometry, matrix, and surface chemistry.

These trends establish some preliminary guidelines for future drug delivery particle design. However, the studies presented here represent only a tiny fraction of the work required to truly define the role of non-spherical particles as drug delivery carriers. Many studies have explored only changes in particle AR or compared a single non-spherical geometry to a spherical control. These studies are often performed with polydisperse particles, some of which change shape dynamically over time (filomicelles, degradable materials), and often do not consider important dynamic conditions when drawing conclusions. As such, there is much work yet to be done.

“Shape” encompasses many more dimensions than a simple change in AR, including local surface roughness, features in all three-dimensions, varied surface curvatures, the potential for creative and diverse biomimicry, numbers of surface appendages, extreme geometries, etc. As a field, we have barely scratched the surface of the potential design possibilities by altering particle shape. The field currently lacks the fabrication techniques required to provide monodisperse, non-spherical particles and needed to design particles with limitless creativity in all three dimensions. However, appropriate computational models can provide preliminary insight into the effects of more extreme particle geometries. We need more studies to make conclusions about how shape and zwitterionic surfaces work together; there is high potential in a combination of shape that maximizes surface interactions (such as a disk) and a moiety that protects against opsonization and hence RES clearance while maintaining high binding affinities. While there are clear indications that particle shape is important, particle behavior during each biological step requires further exploration, preferably in a standardized, high-throughput, physiologically relevant approach. From these sorts of normalized studies, true guidelines for particle geometry can be established, which can be utilized for *a priori* design of particulate carriers optimized for particular disease conditions. Targeting shape for a desired physiological destination continues to hold great potential to increase the efficacy of future drug delivery systems.

## Acknowledgments

This work was funded by NSF CAREER (CBET1054352) and NIH R01 (HL115138) grants to O.E.A.

## Abbreviations

<b>EC</b>	Endothelial Cell
<b>EPR</b>	enhanced permeability and retention
<b>RES</b>	reticuloendothelial system
<b>RBC</b>	red blood cell
<b>AR</b>	aspect ratio
<b>PS</b>	polystyrene
<b>NP</b>	nanoparticle
<b>PLGA</b>	poly(lactic-co-glycolic acid)
<b>CAM</b>	cell adhesion molecule
<b>PEG</b>	polyethylene glycol
<b>VTCs</b>	vascular targeted carriers
<b>CFL</b>	cell-free layer
<b>HUVEC</b>	human umbilical cord endothelial cells
<b>DOX</b>	Doxorubicin
<b>ESD</b>	Equivalent spherical diameter
<b>ICAM-1</b>	Intercellular Adhesion Molecule-1
<b>TfR</b>	transferrin receptor
<b>BSA</b>	Bovine Serum Albumin

## REFERENCES

1. Brannon-Peppas L, Blanchette JO. Nanoparticle and Targeted Systems for Cancer Therapy. *Adv. Drug Deliv. Rev.* 2012; 6:206–212.
2. Faraji AH, Wipf P. Nanoparticles in Cellular Drug Delivery. *Bioorg. Med. Chem.* 2009; 17:2950–2962. [PubMed: 19299149]
3. Misset JL, Dieras V, Gruia G, Bourgeois H, Cvitkovic E, Kalla S, Bozec L, Beuzeboc P, Jasmin C, Aussen JP, Riva A, Azli N, Pouillart P. Original Article Dose-Finding Study of Docetaxel and Doxorubicin in First-Line Treatment of. *Ann. Oncol.* 1999; 10:553–560. [PubMed: 10416005]
4. Torchilin VP. Multifunctional Nanocarriers. *Adv. Drug Deliv. Rev.* 2006; 58:1532–1555. [PubMed: 17092599]
5. Santos LA, Akil EM. Drug Delivery Formulations of Ordered and Nonordered Mesoporous Silica: Comparison of Three Drug Loading Methods. *J. Pharm. Sci.* 2011; 100:3294–3306. [PubMed: 21520084]
6. Zhang L, Gu FX, Chan JM, Wang AZ, Langer RS, Farokhzad OC. Nanoparticles in Medicine : Therapeutic Applications and Developments. *Clin. Pharmacol. Ther.* 2008; 83:761–769. [PubMed: 17957183]

7. Charoenphol P, Mocherla S, Bouis D, Namdee K, Pinsky DJ, Eniola-Adefeso O. Targeting Therapeutics to the Vascular Wall in Atherosclerosis-Carrier Size Matters. *Atherosclerosis*. 2011; 217:364–370. [PubMed: 21601207]
8. Jain RK, Stylianopoulos T. Delivering Nanomedicine to Solid Tumors. *Nat. Rev. Clin. Oncol.* 2010; 7:653–664. [PubMed: 20838415]
9. Nel AE, Mädler L, Velegol D, Xia T, Hoek EMV, Somasundaran P, Klaessig F, Castranova V, Thompson M. Understanding Biophysicochemical Interactions at the Nano-Bio Interface. *Nat. Mater.* 2009; 8:543–557. [PubMed: 19525947]
10. Owens DE, Peppas Na. Opsonization, Biodistribution, and Pharmacokinetics of Polymeric Nanoparticles. *Int. J. Pharm.* 2006; 307:93–102. [PubMed: 16303268]
11. Jiskoot W, van Schie RMF, Carstens MG, Schellekens H. Immunological Risk of Injectable Drug Delivery Systems. *Pharm. Res.* 2009; 26:1303–1314. [PubMed: 19247815]
12. Goldberg M, Langer R, Jia X. Nanostructured Materials for Applications in Drug Delivery and Tissue Engineering. *J. Biomater. Sci. Polym. Ed.* 2007; 18:241–268. [PubMed: 17471764]
13. Yoo J-W, Doshi N, Mitragotri S. Adaptive Micro and Nanoparticles: Temporal Control over Carrier Properties to Facilitate Drug Delivery. *Adv. Drug Deliv. Rev.* 2011; 63:1247–1256. [PubMed: 21605607]
14. Doane T, Burda C. Nanoparticle Mediated Non-Covalent Drug Delivery. *Adv. Drug Deliv. Rev.* 2013; 65:607–621. [PubMed: 22664231]
15. Albanese A, Tang PS, Chan WCW. The Effect of Nanoparticle Size, Shape, and Surface Chemistry on Biological Systems. *Annu. Rev. Biomed. Eng.* 2012; 14:1–16. [PubMed: 22524388]
16. Merkel TJ, Chen K, Jones SW, Pandya Aa, Tian S, Napier ME, Zamboni WE, DeDimone JM. The Effect of Particle Size on the Biodistribution of Low-Modulus Hydrogel PRINT Particles. *J. Control. Release.* 2012; 162:37–44. [PubMed: 22705460]
17. Devarajan PV, Jindal AB, Patil RR, Mulla F, Gaikwad RV, Samad A. Particle Shape: A New Design Parameter for Passive Targeting in Splenotropic Drug Delivery. *J. Pharm. Sci.* 2010; 99:2576–2581. [PubMed: 20091830]
18. Toy R, Hayden E, Shoup C, Baskaran H, Karathanasis E. The Effects of Particle Size, Density and Shape on Margination of Nanoparticles in Microcirculation. *Nanotechnology.* 2011; 22:115101. [PubMed: 21387846]
19. Charoenphol P, Huang RB, Eniola-Adefeso O. Potential Role of Size and Hemodynamics in the Efficacy of Vascular-Targeted Spherical Drug Carriers. *Biomaterials.* 2010; 31:1392–1402. [PubMed: 19954839]
20. Chithrani BD, Ghazani Aa, Chan WCW. Determining the Size and Shape Dependence of Gold Nanoparticle Uptake into Mammalian Cells. *Nano Lett.* 2006; 6:662–668. [PubMed: 16608261]
21. Doshi N, Mitragotri S. Macrophages Recognize Size and Shape of Their Targets. *PLoS One.* 2010; 5
22. Mitragotri S, Lahann J. Physical Approaches to Biomaterial Design. *Nat. Mater.* 2009; 8:15–23. [PubMed: 19096389]
23. Tao L, Hu W, Liu Y, Huang G, Sumer BD, Gao J. Shape-Specific Polymeric Nanomedicine: Emerging Opportunities and Challenges. *Exp. Biol. Med.(Maywood).* 2011; 236:20–29. [PubMed: 21239732]
24. Decuzzi P, Pasqualini R, Arap W, Ferrari M. Intravascular Delivery of Particulate Systems: Does Geometry Really Matter? *Pharm. Res.* 2009; 26:235–243. [PubMed: 18712584]
25. Garcia A, Mack P, Williams S, Fromen C, Shen T, Tully J, Pillai J, Kuehl P, Napier M, Desimone JM, Maynor BW. Microfabricated Engineered Particle Systems for Respiratory Drug Delivery and Other Pharmaceutical Applications. *J. Drug Deliv.* 2012; 2012
26. Champion, Ja; Katare, YK.; Mitragotri, S. Making Polymeric Micro- and Nanoparticles of Complex Shapes. *Proc. Natl. Acad. Sci. U. S. A.* 2007; 104:11901–11904. [PubMed: 17620615]
27. Tao L, Zhao XM, Gao JM, Hu W. Lithographically Defined Uniform Worm-Shaped Polymeric Nanoparticles. *Nanotechnology.* 2010; 21:095301. [PubMed: 20110578]
28. Glangchai LC, Caldorera-Moore M, Shi L, Roy K. Nanoimprint Lithography Based Fabrication of Shape-Specific, Enzymatically-Triggered Smart Nanoparticles. *J. Control. Release.* 2008; 125:263–272. [PubMed: 18053607]

29. Acharya G, Shin CS, McDermott M, Mishra H, Park H, Kwon IC, Park K. The Hydrogel Template Method for Fabrication of Homogeneous Nano/microparticles. *J. Control. Release.* 2010; 141:314–319. [PubMed: 19822178]
30. Rolland JP, Maynor BW, Euliss LE, Exner AE, Denison GM, Desimone JM. Direct Fabrication and Harvesting of Monodisperse, Shape-Specific Nanobiomaterials. *J. Am. Chem. Soc.* 2005; 127:10096–10100. [PubMed: 16011375]
31. Dendukuri D, Gu SS, Pregibon DC, Hatton TA, Doyle PS. Stop-Flow Lithography in a Microfluidic Device. *Lab Chip.* 2007; 7:818–828. [PubMed: 17593999]
32. Suh SK, Yuet K, Hwang DK, Bong KW, Doyle PS, Hatton TA. Synthesis of Nonspherical Superparamagnetic Particles: In Situ Coprecipitation of Magnetic Nanoparticles in Microgels Prepared by Stop-Flow Lithography. *J. Am. Chem. Soc.* 2012; 134:7337–7343. [PubMed: 22462394]
33. Lu Z, Qiao Y, Zheng XT, Chan-Park MB, Li CM. Effect of Particle Shape on Phagocytosis of CdTe Quantum Dot–cystine Composites. *Medchemcomm.* 2010; 1:84.
34. Champion, Ja; Mitragotri, S. Shape Induced Inhibition of Phagocytosis of Polymer Particles. *Pharm. Res.* 2009; 26:244–249. [PubMed: 18548338]
35. Lin S-Y, Hsu W-H, Lo J-M, Tsai H-C, Hsiue G-H. Novel Geometry Type of Nanocarriers Mitigated the Phagocytosis for Drug Delivery. *J. Control. Release.* 2011; 154:84–92. [PubMed: 21565231]
36. Arnida, Janát-Amsbury MM, Ray a, Peterson CM, Ghandehari H. Geometry and Surface Characteristics of Gold Nanoparticles Influence Their Biodistribution and Uptake by Macrophages. *Eur. J. Pharm. Biopharm.* 2011; 77:417–423. [PubMed: 21093587]
37. Sharma G, Valenta DT, Altman Y, Harvey S, Xie H, Mitragotri S, Smith JW. Polymer Particle Shape Independently Influences Binding and Internalization by Macrophages. *J. Control. Release.* 2010; 147:408–412. [PubMed: 20691741]
38. Champion, Ja; Mitragotri, S. Role of Target Geometry in Phagocytosis. *Proc. Natl. Acad. Sci. U. S. A.* 2006; 103:4930–4934. [PubMed: 16549762]
39. Geng Y, Dalhaimer P, Cai S, Tsai R, Tewari M, Minko T, Discher DE. Shape Effects of Filaments versus Spherical Particles in Flow and Drug Delivery. *Nat. Nanotechnol.* 2007; 2:249–255. [PubMed: 18654271]
40. Schinwald A, Chernova T, Donaldson K. Use of Silver Nanowires to Determine Thresholds for Fibre Length-Dependent Pulmonary Inflammation and Inhibition of Macrophage Migration in Vitro. *Part. Fibre Toxicol.* 2012; 9:47. [PubMed: 23199075]
41. Dasgupta S, Auth T, Gompper G. Shape and Orientation Matter for the Cellular Uptake of Nonspherical Particles. *Nano Lett.* 2014; 14:687–693. [PubMed: 24383757]
42. Bartneck M, Keul Ha, Zwadlo-Klarwasser G, Groll J. Phagocytosis Independent Extracellular Nanoparticle Clearance by Human Immune Cells. *Nano Lett.* 2010; 10:59–63. [PubMed: 19994869]
43. Chen J, Kozlovskaya V, Goins A, Campos-Gomez J, Saeed M, Kharlampieva E. Biocompatible Shaped Particles from Dried Multilayer Polymer Capsules. *Biomacromolecules.* 2013; 14:3830–3841. [PubMed: 24063405]
44. Müller KH, Motskin M, Philpott AJ, Routh AF, Shanahan CM, Duer MJ, Skepper JN. The Effect of Particle Agglomeration on the Formation of a Surface-Connected Compartment Induced by Hydroxyapatite Nanoparticles in Human Monocyte-Derived Macrophages. *Biomaterials.* 2014; 35:1074–1088. [PubMed: 24183166]
45. Mebius RE, Kraal G. Structure and Function of the Spleen. *Nat. Rev. Immunol.* 2005; 5:606–616. [PubMed: 16056254]
46. Cesta MF. Normal Structure, Function, and Histology of the Spleen. *Toxicol. Pathol.* 2006; 34:455–465. [PubMed: 17067939]
47. Moghimi SM. Mechanisms of Splenic Clearance of Blood Cells and Particles: Towards Development of New Splenotropic Agents. *Adv. Drug Deliv. Rev.* 1995; 17:103–115.
48. Park J-H, von Maltzahn G, Zhang L, Schwartz MP, Ruoslahti E, Bhatia SN, Sailor MJ. Magnetic Iron Oxide Nanoworms for Tumor Targeting and Imaging. *Adv. Mater.* 2008; 20:1630–1635. [PubMed: 21687830]

49. Akiyama Y, Mori T, Katayama Y, Niidome T. Conversion of Rod-Shaped Gold Nanoparticles to Spherical Forms and Their Effect on Biodistribution in Tumor-Bearing Mice. *Nanoscale Res. Lett.* 2012; 7:565. [PubMed: 23050635]
50. Longmire M, Choyke PL, Kobayashi H. Clearance Properties of Nano-Sized Particles and Molecules as Imaging Agents: Considerations and Caveats. *Nanomedicine(Lond)*. 2008; 3:703–717. [PubMed: 18817471]
51. Boulikas T. Clinical Overview on Lipoplatin: A Successful Liposomal Formulation of Cisplatin. *Expert Opin. Investig. Drugs*. 2009; 18:1197–1218.
52. Tomlinson E. Theory and Practice of Site-Specific Drug Delivery. *Advanced Drug Delivery Reviews*. 1987; 1:87–198.
53. Bilzer M, Roggel F, Gerbes AL. Role of Kupffer Cells in Host Defense and Liver Disease. *Liver International*. 2006; 26:1175–1186. [PubMed: 17105582]
54. Perry JL, Reuter KG, Kai MP, Herlihy KP, Jones SW, Luft JC, Napier M, Bear JE, DeSimone JM. PEGylated PRINT Nanoparticles: The Impact of PEG Density on Protein Binding, Macrophage Association, Biodistribution, and Pharmacokinetics. *Nano Lett.* 2012; 12:5304–5310. [PubMed: 22920324]
55. Decuzzi P, Godin B, Tanaka T, Lee S-Y, Chiappini C, Liu X, Ferrari M. Size and Shape Effects in the Biodistribution of Intravascularly Injected Particles. *J. Control. Release*. 2010; 141:320–327. [PubMed: 19874859]
56. Park JH, Von Maltzahn G, Zhang L, Derfus AM, Simberg D, Harris TJ, Ruoslahti E, Bhatia SN, Sailor MJ. Systematic Surface Engineering of Magnetic Nanoworms for in Vivo Tumor Targeting. *Small*. 2009; 5:694–700. [PubMed: 19263431]
57. Muro S, Garnacho C, Champion JA, Leferovich J, Gajewski C, Schuchman EH, Mitragotri S, Muzykantov VR. Control of Endothelial Targeting and Intracellular Delivery of Therapeutic Enzymes by Modulating the Size and Shape of ICAM-1-Targeted Carriers. *Mol. Ther.* 2008; 16:1450–1458. [PubMed: 18560419]
58. Zhang W, Sun J, Liu Y, Tao M, Ai X, Su X, Cai C, Tang Y, Feng Z, Yan X, Chen G, He Z. PEG-Stabilized Bilayer Nanodisks As Carriers for Doxorubicin Delivery. *Mol. Pharm.* 2014; 11:3279–3290. [PubMed: 24754897]
59. Floyd J, Mirza I, Sachs B, Perry MC. Hepatotoxicity of Chemotherapy. *Semin. Oncol.* 2006; 33:50–67. [PubMed: 16473644]
60. Zalipsky S. Chemistry of Polyethylene Glycol Conjugates with Biologically Active Molecules. *Adv. Drug Deliv. Rev.* 1995; 16:157–182.
61. Rahme K, Chen L, Hobbs RG, Morris Ma, O'Driscoll C, Holmes JD. PEGylated Gold Nanoparticles: Polymer Quantification as a Function of PEG Lengths and Nanoparticle Dimensions. *RSC Adv.* 2013; 3:6085.
62. Christian DA, Cai S, Garbuzenko OB, Harada T, Zajac AL, Minko T, Discher DE. Flexible Filaments for in Vivo Imaging and Delivery: Persistent Circulation of Filomicelles Opens the Dosage Window for Sustained Tumor Shrinkage. *Mol. Pharm.* 2009; 6:1343–1352. [PubMed: 19249859]
63. Champion JA, Mitragotri S. Shape Induced Inhibition of Phagocytosis of Polymer Particles. *Pharm. Res.* 2009; 26:244–249. [PubMed: 18548338]
64. Gormley AJ, Greish K, Ray A, Robinson R, Gustafson JA, Ghandehari H. Gold Nanorod Mediated Plasmonic Photothermal Therapy: A Tool to Enhance Macromolecular Delivery. *Int. J. Pharm.* 2011; 415:315–318. [PubMed: 21669265]
65. Huang X, Li L, Liu T, Hao N, Liu H, Chen D, Tang F. The Shape Effect of Mesoporous Silica Nanoparticles on Biodistribution, Clearance, and Biocompatibility in Vivo. *ACS Nano*. 2011; 5:5390–5399. [PubMed: 21634407]
66. Lai MH, Jeong JH, Devolder RJ, Brockman C, Schroeder C, Kong H. Ellipsoidal Polyaspartamide Polymersomes with Enhanced Cell-Targeting Ability. *Adv. Funct. Mater.* 2012; 22:3239–3246. [PubMed: 23976892]
67. Keefe AJ, Jiang S. Poly(zwitterionic)protein Conjugates Offer Increased Stability without Sacrificing Binding Affinity or Bioactivity. *Nat. Chem.* 2011; 4:59–63. [PubMed: 22169873]

68. Lee S-Y, Ferrari M, Decuzzi P. Shaping Nano-/micro-Particles for Enhanced Vascular Interaction in Laminar Flows. *Nanotechnology*. 2009; 20:495101. [PubMed: 19904027]
69. Filipovic N, Kojic M, Ferrari M. Dissipative Particle Dynamics Simulation of Circular and Elliptical Particles Motion in 2D Laminar Shear Flow. *Microfluid. Nanofluidics*. 2011; 10:1127–1134.
70. Lee SY, Ferrari M, Decuzzi P. Design of Bio-Mimetic Particles with Enhanced Vascular Interaction. *J. Biomech*. 2009; 42:1885–1890. [PubMed: 19523635]
71. Ehd, Gavze; Shapiro, Michael. Motion of Inertial Spheroidal Particles in a Shear Flow near a Solid Wall with Special Application to Aerosol Transport in Microgravity. *J. Fluid Mech*. 1998; 371:59–79.
72. Mody NA, King MR. Three-Dimensional Simulations of a Platelet-Shaped Spheroid near a Wall in Shear Flow. *Phys. Fluids*. 2005; 17:1–12.
73. Pozrikidis C. Orbiting Motion of a Freely Suspended Spheroid near a Plane Wall. *Journal of Fluid Mechanics*. 2005; 541:105.
74. Broday D, Shapiro M, Fichman M, Gutfinger C. Motion of Micron Spheroidal Particles in Vertical Shear Flows. *Journal of Aerosol Science*. 1997; 28:1353.
75. Gentile F, Chiappini C, Fine D, Bhavane RC, Peluccio MS, Cheng MMC, Liu X, Ferrari M, Decuzzi P. The Effect of Shape on the Margination Dynamics of Non-Neutrally Buoyant Particles in Two-Dimensional Shear Flows. *J. Biomech*. 2008; 41:2312–2318. [PubMed: 18571181]
76. Doshi N, Prabhakarandian B, Rea-Ramsey A, Pant K, Sundaram S, Mitragotri S. Flow and Adhesion of Drug Carriers in Blood Vessels Depend on Their Shape: A Study Using Model Synthetic Microvascular Networks. *J. Control. Release*. 2010; 146:196–200. [PubMed: 20385181]
77. Lee SY, Ferrari M, Decuzzi P. Shaping Nano-/micro-Particles for Enhanced Vascular Interaction in Laminar Flows. *Nanotechnology*. 2009; 20:495101. [PubMed: 19904027]
78. Eckstein EC, Tilles AW, Millero FJ. Conditions for the Occurrence of Large near-Wall Excesses of Small Particles during Blood Flow. *Microvasc. Res*. 1988; 36:31–39. [PubMed: 3185301]
79. Lee T-R, Choi M, Kopacz AM, Yun S-H, Liu WK, Decuzzi P. On the near-Wall Accumulation of Injectable Particles in the Microcirculation: Smaller Is Not Better. *Sci. Rep*. 2013; 3:2079. [PubMed: 23801070]
80. Tilles AW, Eckstein EC. The near-Wall Excess of Platelet-Sized Particles in Blood Flow: Its Dependence on Hematocrit and Wall Shear Rate. *Microvasc. Res*. 1987; 33:211–223. [PubMed: 3587076]
81. Namdee K, Thompson AJ, Charoenphol P, Eniola-Adefeso O. Margination Propensity of Vascular-Targeted Spheres from Blood Flow in a Microfluidic Model of Human Microvessels. *Langmuir*. 2013; 29:2530–2535. [PubMed: 23363293]
82. Thompson AJ, MASTRIA EM, Eniola-Adefeso O. The Margination Propensity of Ellipsoidal Micro/nanoparticles to the Endothelium in Human Blood Flow. *Biomaterials*. 2013; 34:5863–5871. [PubMed: 23642534]
83. Namdee K, Thompson AJ, Golinski A, Mocherla S, Bouis D, Eniola-Adefeso O. In Vivo Evaluation of Vascular-Targeted Spheroidal Microparticles for Imaging and Drug Delivery Application in Atherosclerosis. *Atherosclerosis*. 2014; 237:279–286. [PubMed: 25286447]
84. Müller K, Fedosov Da, Gompper G. Margination of Micro- and Nano-Particles in Blood Flow and Its Effect on Drug Delivery. *Sci. Rep*. 2014; 4:4871. [PubMed: 24786000]
85. Shah S, Liu Y, Hu W, Gao J. Modeling Particle Shape-Dependent Dynamics in Nanomedicine. *J. Nanosci. Nanotechnol*. 2011; 11:919–928. [PubMed: 21399713]
86. Kolhar P, Anselmo AC, Gupta V, Pant K, Prabhakarandian B, Ruoslahti E, Mitragotri S. Using Shape Effects to Target Antibody-Coated Nanoparticles to Lung and Brain Endothelium. *Proc. Natl. Acad. Sci. U. S. A*. 2013; 110:10753–10758. [PubMed: 23754411]
87. Decuzzi P, Ferrari M. The Adhesive Strength of Non-Spherical Particles Mediated by Specific Interactions. *Biomaterials*. 2006; 27:5307–5314. [PubMed: 16797691]
88. Yang K, Ma Y-Q. Computer Simulation of the Translocation of Nanoparticles with Different Shapes across a Lipid Bilayer. *Nat. Nanotechnol*. 2010; 5:579–583. [PubMed: 20657599]
89. Vácha R, Martinez-Veracoechea FJ, Frenkel D. Receptor-Mediated Endocytosis of Nanoparticles of Various Shapes. *Nano Lett*. 2011; 11:5391–5395. [PubMed: 22047641]



90. Decuzzi P, Ferrari M. The Receptor-Mediated Endocytosis of Nonspherical Particles. *Biophys. J.* 2008; 94:3790–3797. [PubMed: 18234813]
91. Bahrami AH. Orientational Changes and Impaired Internalization of Ellipsoidal Nanoparticles by Vesicle Membranes. *Soft Matter.* 2013; 9:8642.
92. Canelas DA, Herlihy KP, Desimone JM. Top-down Particle Fabrication : Control of Size and Shape for Diagnostic Imaging and Drug Delivery. 2009; 1:391–404.
93. Chithrani BD, Chan WCW. Elucidating the Mechanism of Cellular Uptake and Removal of Protein-Coated Gold Nanoparticles of Different Sizes and Shapes. *Nano Lett.* 2007; 7:1542–1550. [PubMed: 17465586]
94. Gratton, SEa; Ropp, Pa; Pohlhaus, PD.; Luft, JC.; Madden, VJ.; Napier, ME.; DeSimone, JM. The Effect of Particle Design on Cellular Internalization Pathways. *Proc. Natl. Acad. Sci. U. S. A.* 2008; 105:11613–11618. [PubMed: 18697944]
95. Yoo J-W, Doshi N, Mitragotri S. Endocytosis and Intracellular Distribution of PLGA Particles in Endothelial Cells: Effect of Particle Geometry. *Macromol. Rapid Commun.* 2010; 31:142–148. [PubMed: 21590886]
96. Shimoni O, Yan Y, Wang Y, Caruso F. Shape-Dependent Cellular Processing of Polyelectrolyte Capsules. *ACS Nano.* 2013; 7:522–530. [PubMed: 23234433]
97. Agarwal R, Singh V, Journey P, Shi L, Sreenivasan SV, Roy K. Mammalian Cells Preferentially Internalize Hydrogel Nanodiscs over Nanorods and Use Shape-Specific Uptake Mechanisms. *Proc. Natl. Acad. Sci. U. S. A.* 2013; 110:17247–17252. [PubMed: 24101456]
98. Huang X, Teng X, Chen D, Tang F, He J. The Effect of the Shape of Mesoporous Silica Nanoparticles on Cellular Uptake and Cell Function. *Biomaterials.* 2010; 31:438–448. [PubMed: 19800115]
99. Meng H, Yang S, Li Z, Xia T, Chen J, Ji Z, Zhang H, Wang X, Lin S, Huang C, Zhou ZH, Zink JJ, Nel AE. Aspect Ratio Determines the Quantity of Mesoporous Silica Nanoparticle Uptake by a Small GTPase-Dependent Macropinocytosis Mechanism. *ACS Nano.* 2011; 5:4434–4447. [PubMed: 21563770]
100. Herd H, Daum N, Jones AT, Huwer H, Ghandehari H, Lehr C-M. Nanoparticle Geometry and Surface Orientation Influence Mode of Cellular Uptake. *ACS Nano.* 2013; 7:1961–1973. [PubMed: 23402533]
101. She S, Yu D, Han X, Tong W, Mao Z, Gao C. Fabrication of Biconcave Discoidal Silica Capsules and Their Uptake Behavior by Smooth Muscle Cells. *J. Colloid Interface Sci.* 2014; 426:124–130. [PubMed: 24863774]
102. Zhang W, Tong L, Yang C. Cellular Binding and Internalization of Functionalized Silicon Nanowires. *Nano Lett.* 2012; 12:1002–1006. [PubMed: 22268425]
103. Underhill DM, Goodridge HS. Information Processing during Phagocytosis. *Nat. Rev. Immunol.* 2012; 12:492–502. [PubMed: 22699831]
104. Rejman J, Oberle V, Zuhorn IS, Hoekstra D. Size-Dependent Internalization of Particles via the Pathways of Clathrin- and Caveolae-Mediated Endocytosis. *Biochem. J.* 2004; 377:159–169. [PubMed: 14505488]
105. Conner SD, Schmid SL. Regulated Portals of Entry into the Cell. *Nature.* 2003; 422:37–44. [PubMed: 12621426]
106. Chu KS, Hasan W, Rawal S, Walsh MD, Enlow EM, Luft JC, Bridges AS, Kuijter JL, Napier ME, Zamboni WC, DeSimone JM. Plasma, Tumor and Tissue Pharmacokinetics of Docetaxel Delivered via Nanoparticles of Different Sizes and Shapes in Mice Bearing SKOV-3 Human Ovarian Carcinoma Xenograft. *Nanomedicine.* 2013; 9:686–693. [PubMed: 23219874]
107. Chauhan VP, Popovi Z, Chen O, Cui J, Fukumura D, Bawendi MG, Jain RK. Fluorescent Nanorods and Nanospheres for Real-Time In Vivo Probing of Nanoparticle Shape-Dependent Tumor Penetration. *Angew. Chemie.* 2011; 123:11619–11622.
108. Smith BR, Kempen P, Bouley D, Xu A, Liu Z, Melosh N, Dai H, Sinclair R, Gambhir SS. Shape Matters: Intravital Microscopy Reveals Surprising Geometrical Dependence for Nanoparticles in Tumor Models of Extravasation. *Nano Lett.* 2012; 12:3369–3377. [PubMed: 22650417]
109. Yang L, Fassihi R. Zero-Order Release Kinetics from a Self-Correcting Floatable Asymmetric Configuration Drug Delivery System. *J. Pharm. Sci.* 1996; 85:170–173. [PubMed: 8683443]

110. Fattahi P, Borhan A, Abidian MR. Microencapsulation of Chemotherapeutics into Monodisperse and Tunable Biodegradable Polymers via Electrified Liquid Jets: Control of Size, Shape, and Drug Release. *Adv. Mater.* 2013; 25:4555–4560. [PubMed: 23824544]
111. Yu D-G, Li X-Y, Wang X, Chian W, Liao Y-Z, Li Y. Zero-Order Drug Release Cellulose Acetate Nanofibers Prepared Using Coaxial Electrospinning. *Cellulose.* 2012; 20:379–389.
112. Heslinga MJ, Willis GM, Sobczynski DJ, Thompson AJ, Eniola-Adefeso O. One-Step Fabrication of Agent-Loaded Biodegradable Microspheroids for Drug Delivery and Imaging Applications. *Colloids Surf. B. Biointerfaces.* 2014; 116:55–62. [PubMed: 24441181]

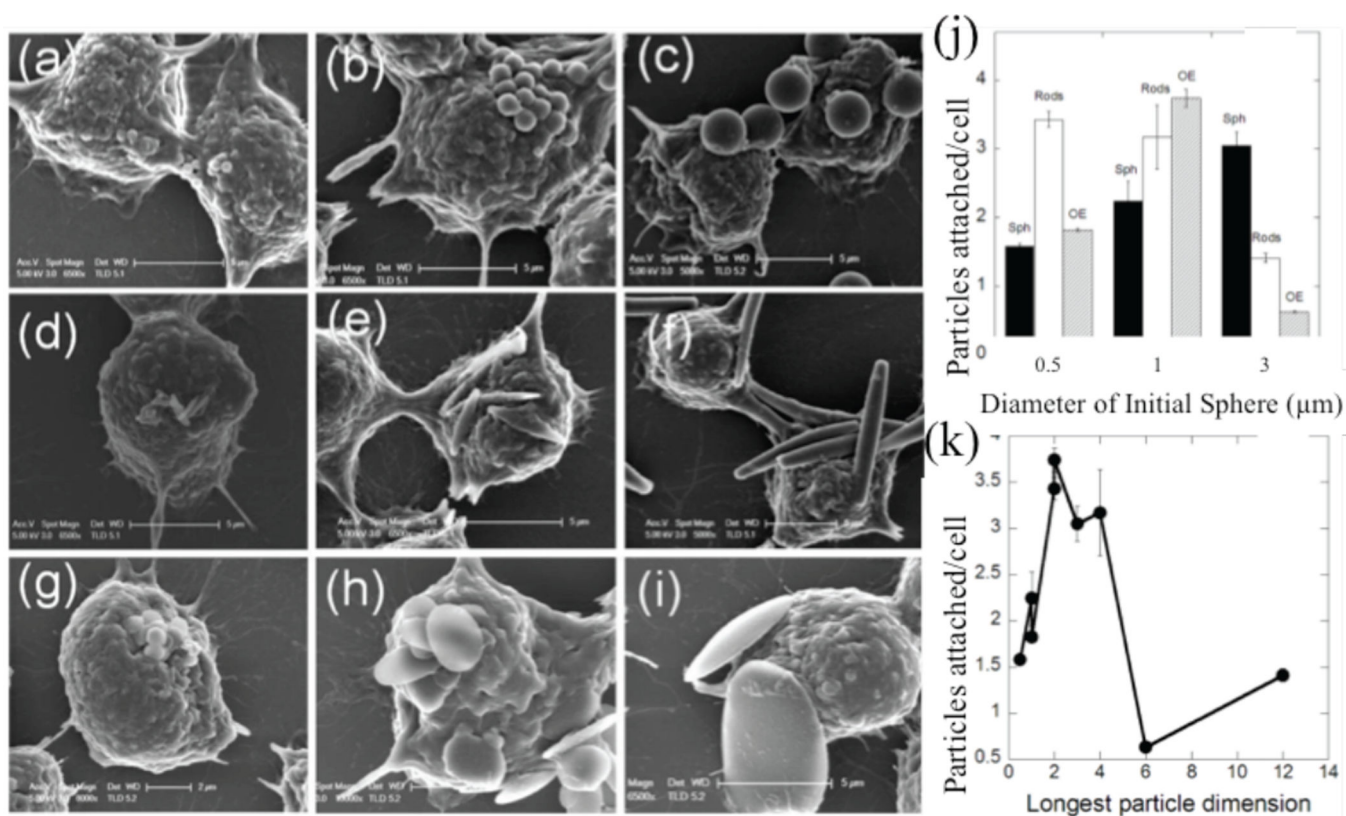


**Figure 1.** Particle shape-dependence of macrophage-particle attachment. SEM images of particle attachment to macrophages including (A–C) spheres, (D–F) rods, and (G–I) disks of ESD (A,D,G) 0.5μm, (B,E,H) 1μm, and (C,F,I) 3 μm. (J) Quantification of attachment densities by shapes and sizes described in (A–I), and attachment propensity of particles by longest particle dimension.<sup>21</sup> Adapted with permission from reference #21. Copyright 2010 Public Library of Science.

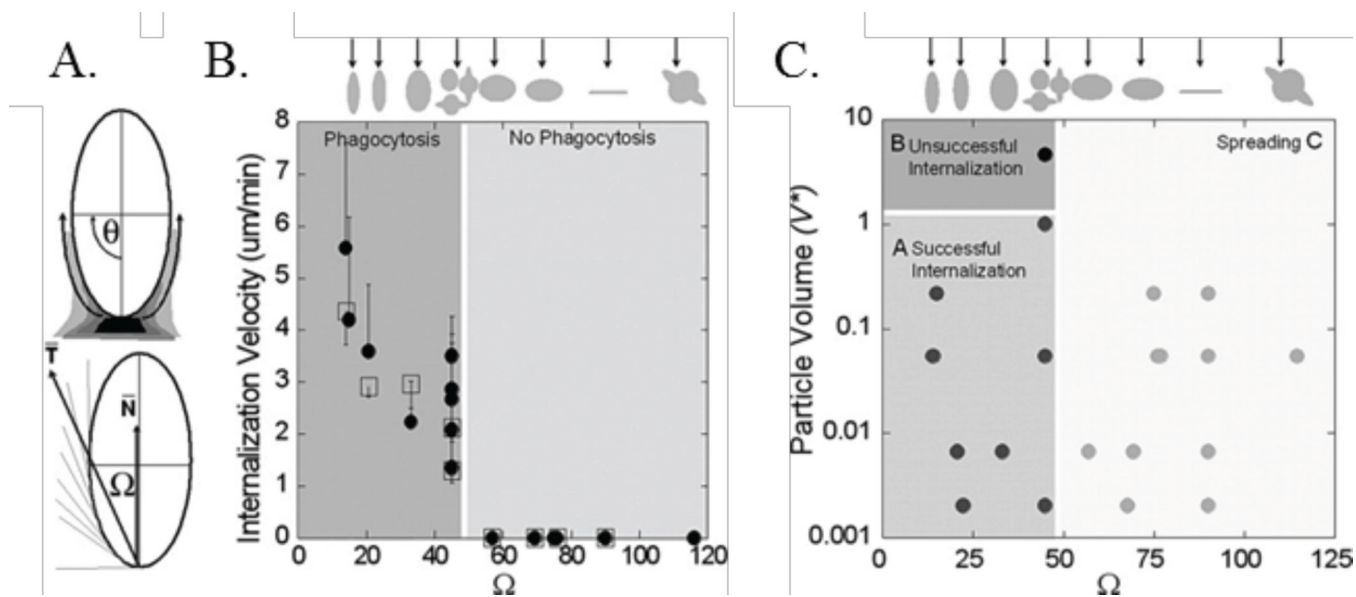


**Figure 2.** The fate of particle-macrophage interactions are controlled by  $\Omega$ . (A) Definition of  $\Omega$ , its relation to (B) internalization velocity, and (C) the resulting phagocytosis phase diagram.<sup>38</sup> Adapted with permission from reference #38. Copyright 2006 National Academy of Sciences, U.S.A.

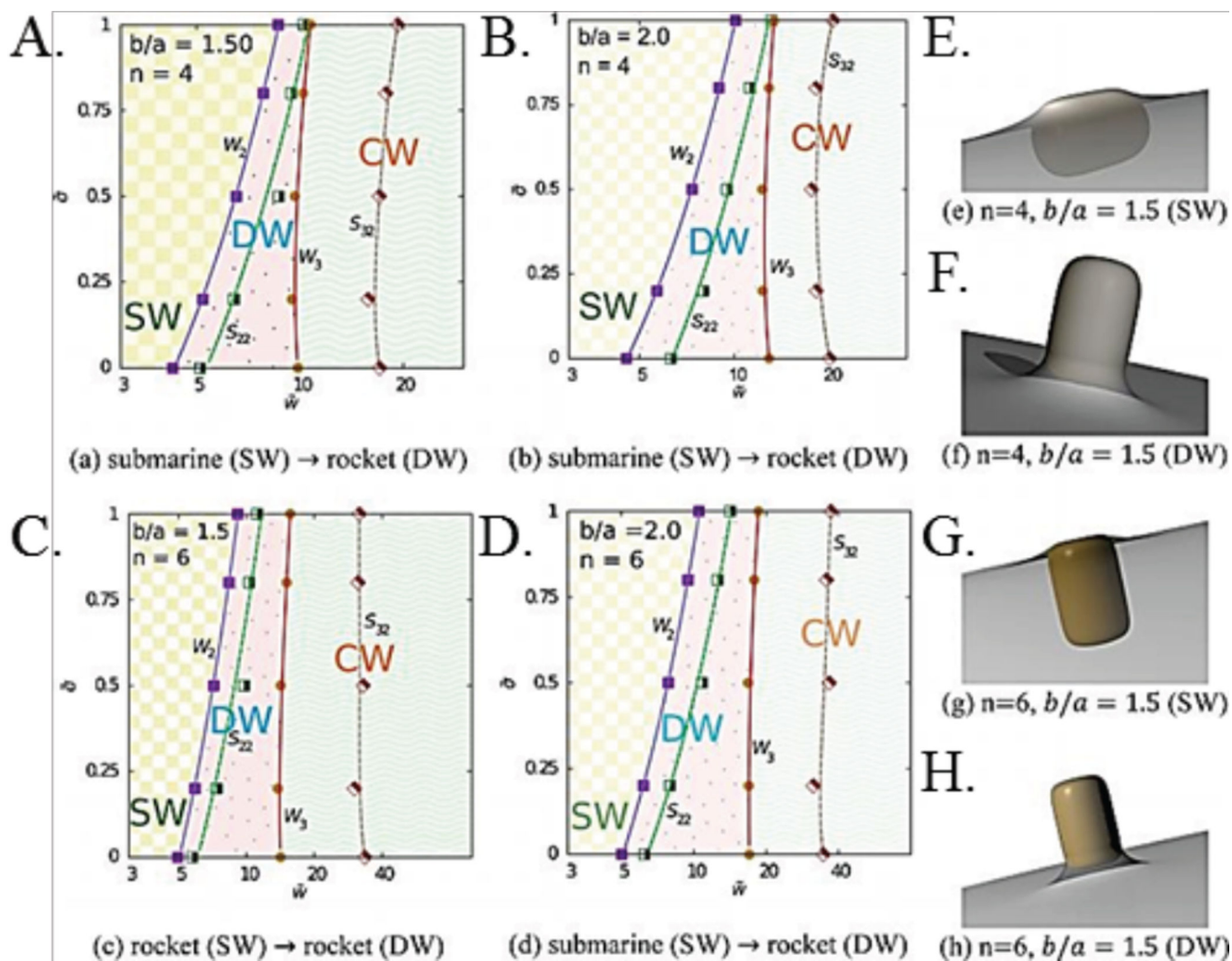


**Figure 3.** (A–D) Phase diagrams of final wrapping state of particles with constant volume and varying AR, adhesion-particle interaction strength (x-axis), and membrane tension (y-axis). Particles are either, deep, shallow, or completely wrapped. The variable  $n$  increases as a particle becomes more like a cylinder and has sharper edges. (E–H) Schematics of shallow and deep wrapping.<sup>41</sup> Adapted with permission from reference #41. Copyright 2014 American Chemical Society.

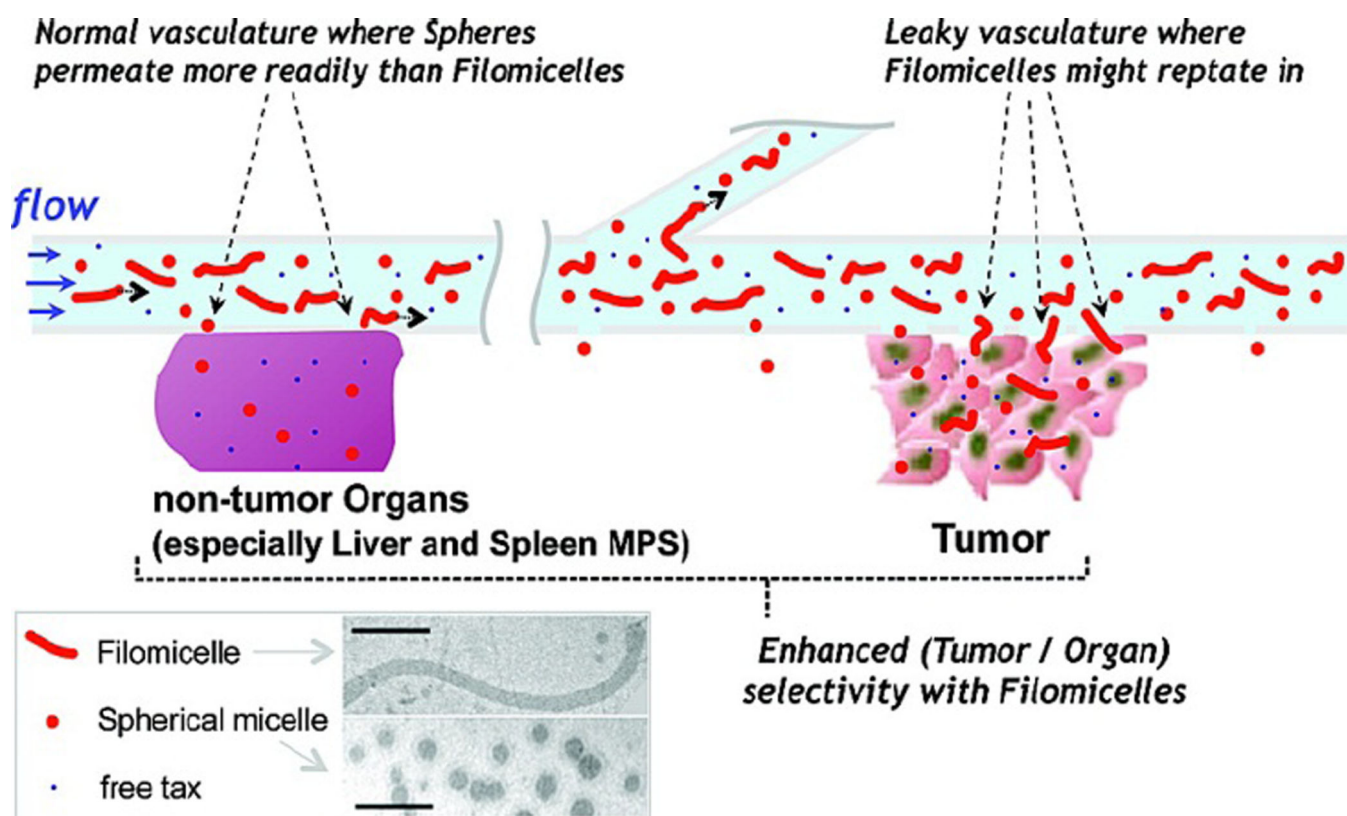


**Figure 4.** Schematic of filomicelle and spherical micelle circulation in tumor models. Filomicelles have superior uptake enhancement in tumor vasculature as compared to healthy vasculature, creating tumor-specific accumulation.<sup>62</sup> Reproduced with permission from reference #62. Copyright 2009 American Chemical Society.

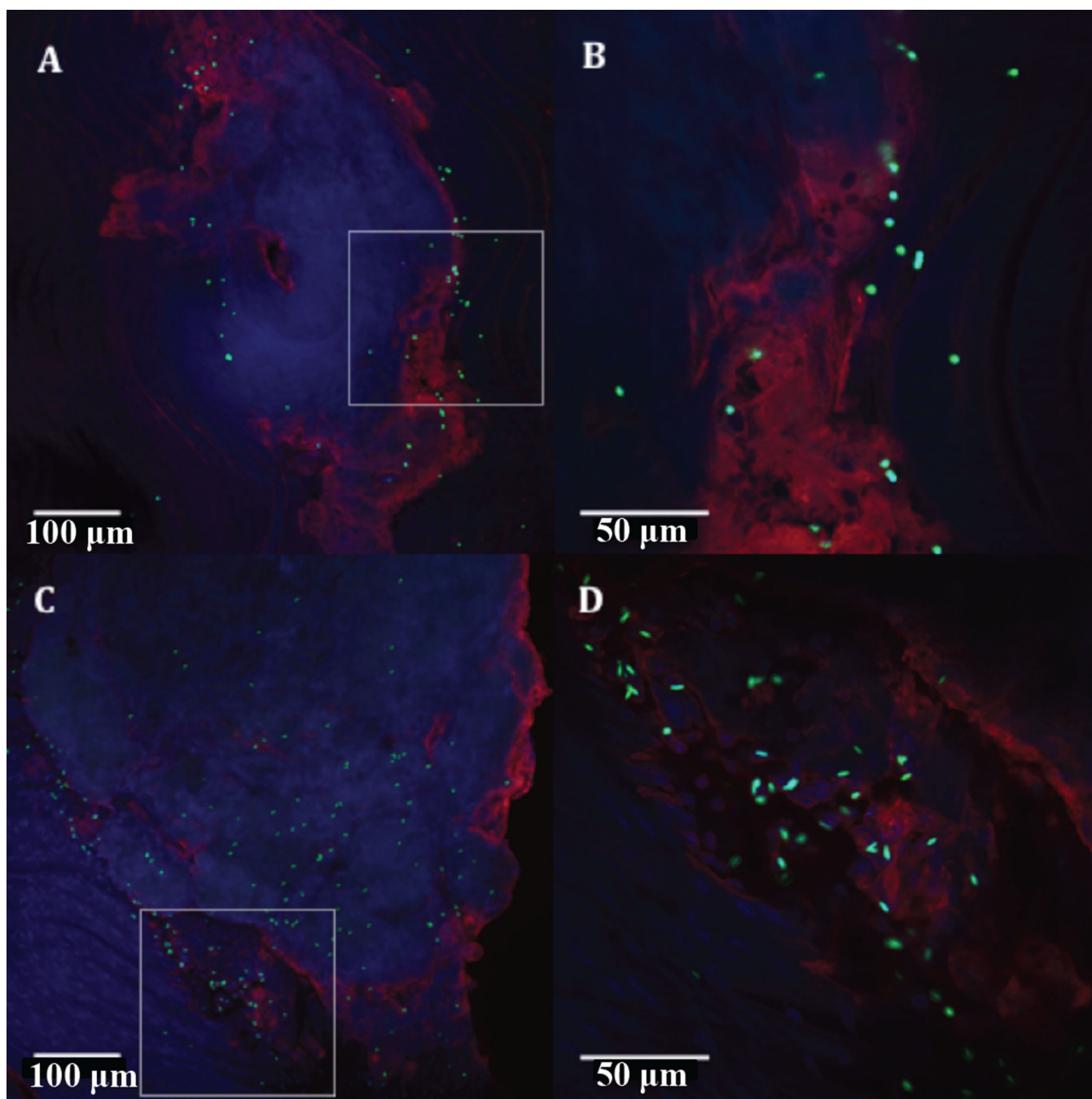


**Figure 5.** Representative images of aortic arch with atherosclerotic plaque with adhesion of 2 μm ESD spheres (A–B) and 2 μm ESD rods (C–D) at 20× and 60× magnification, respectively, qualitatively showing the increased adhesion of rods particularly near the periphery of plaques.<sup>83</sup> Reproduced with permission from reference #83. Copyright 2014 Elsevier Ireland Ltd.

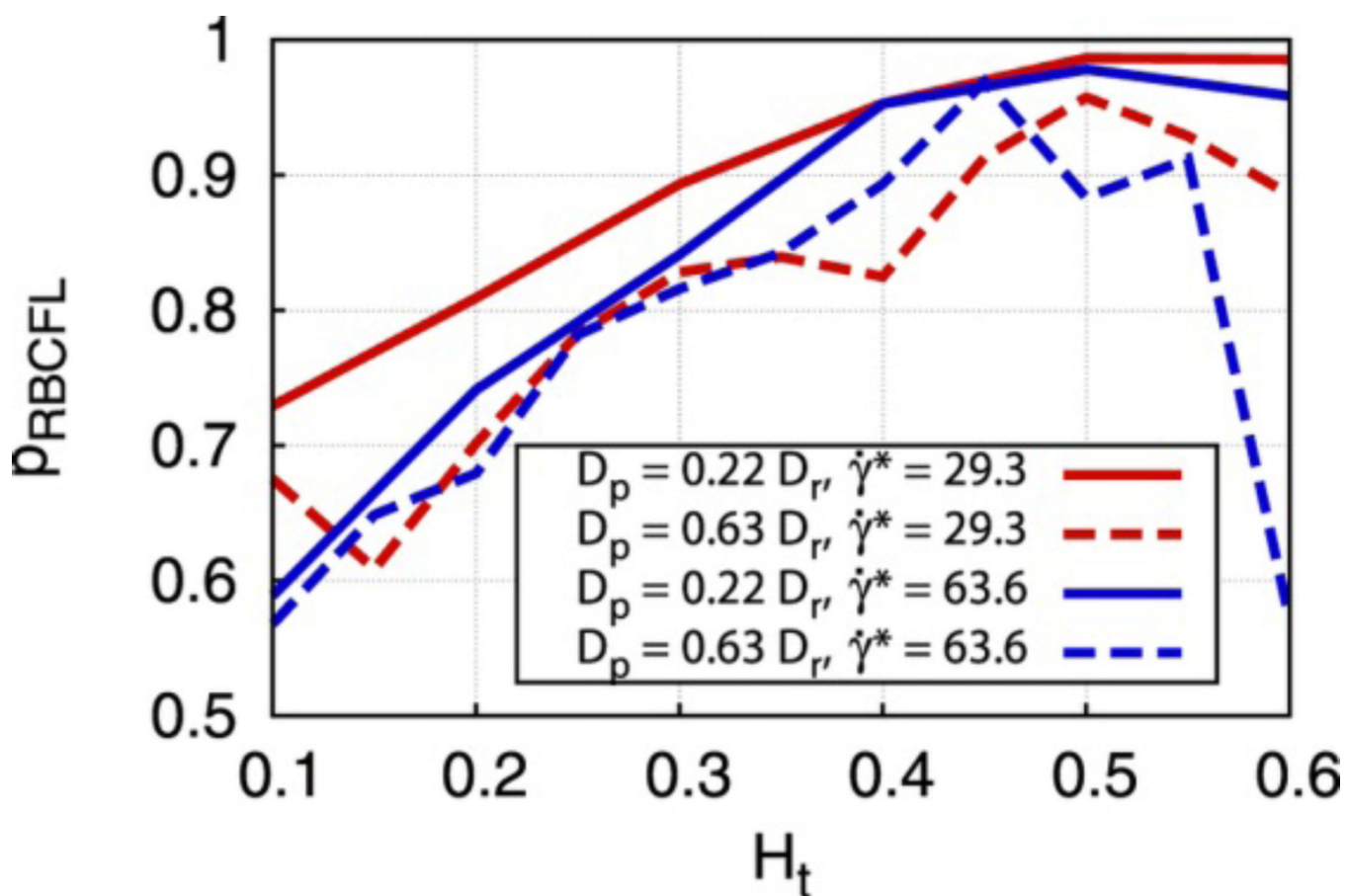


**Figure 6.** Margination probabilities for 2D ellipse-like particles (dashed lines) and circular particles (solid lines). Colors represent different shear rates while the x-axis represents the hematocrit of the flow. Here, the margination of elliptical particles is slightly worse than that of circular particles.<sup>84</sup> Reproduced with permission from reference #84. Copyright 2014 Nature Publishing Group.



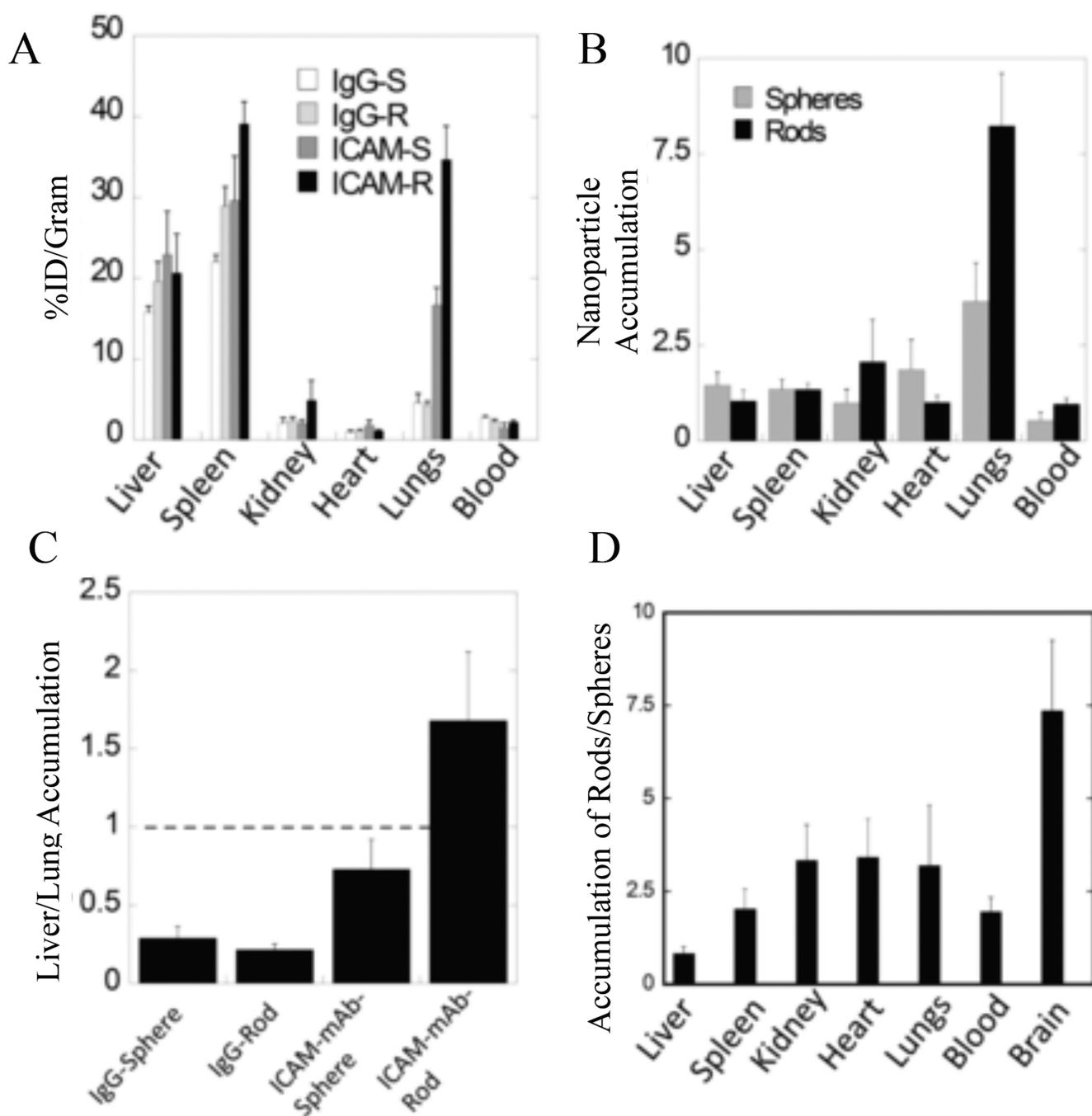


**Figure 7.** Biodistribution of ICAM-1 targeted particles. (A) Distribution of PS ICAM-targeted or IgG-coated spheres and rods and (B) the same data as a ratio of non-specific IgG particle accumulation to specific ICAM-targeted particle accumulation for spheres and rods. (C) Representation of the same data as a ratio of lung to liver accumulation and the resulting (D) ratio of rods to spheres found in each organ.<sup>86</sup> Reproduced with permission from reference #86. Copyright 2013 National Academy of Sciences, U.S.A.

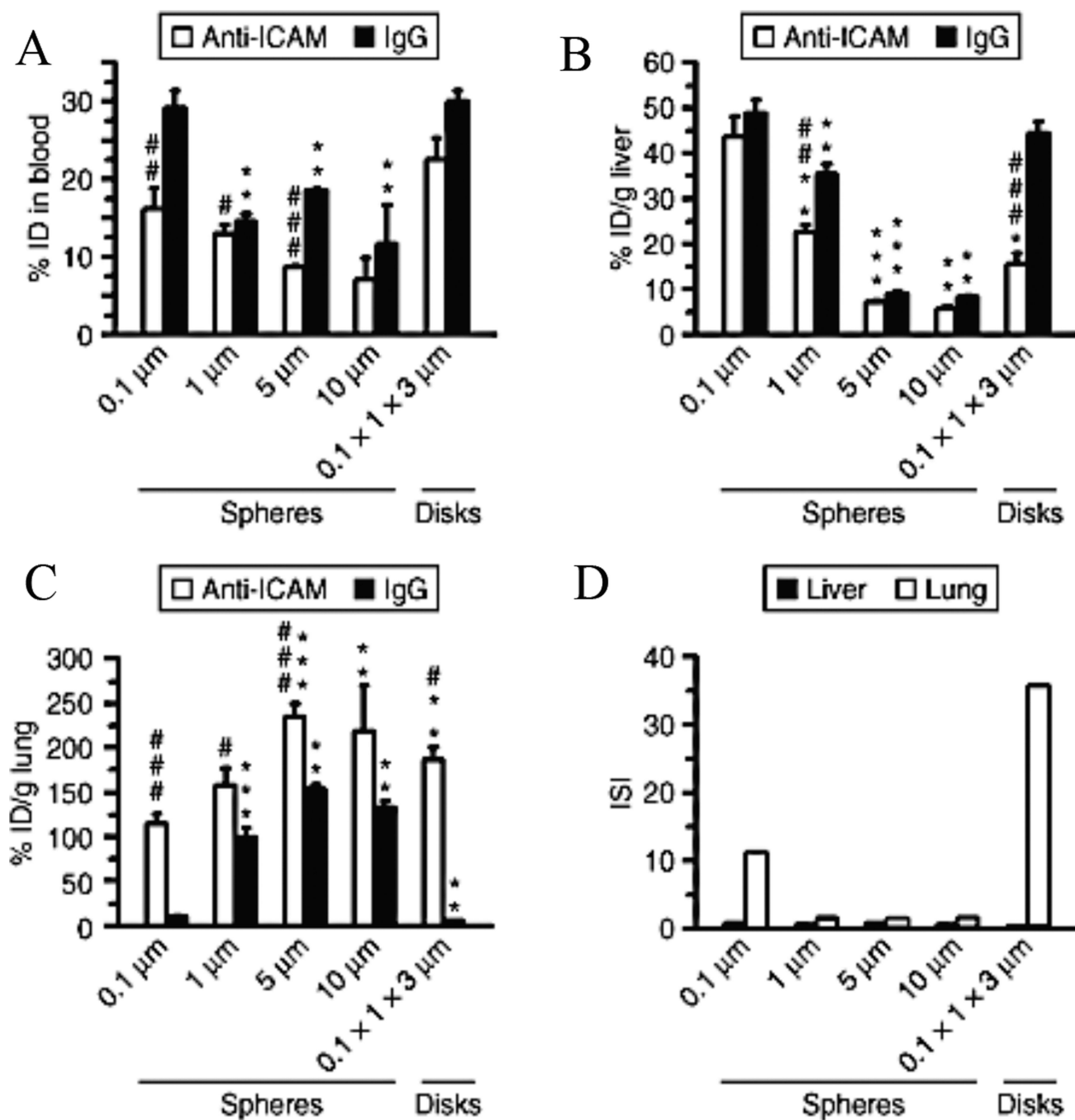


**Figure 8.** Murine biodistribution of PS particles coated with anti-ICAM or non-specific IgG. The accumulation is shown for various geometries in the (A) blood, (B) liver, and (C) lung. (D) The immunospecificity index (ISI) is defined as the ratio of anti-ICAM particle accumulation (targeted) to IgG particle accumulation (non-targeted) and represents the enhancement of specific over non-specific binding.<sup>57</sup> Reproduced with permission from reference #57. Copyright 2008 Nature Publishing Group.

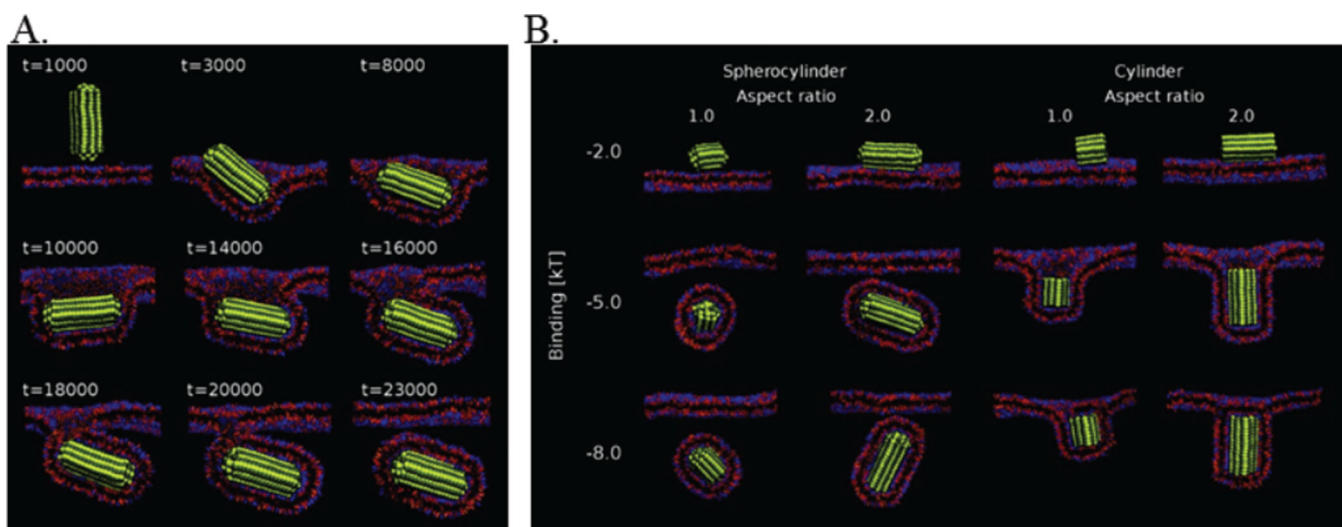


**Figure 9.**

Uptake kinetics and final wrapping state based on AR and binding affinity. (A) Representative snapshots of the endocytosis of a spherocylinder over time. The particle changes orientation during internalization for most favorable energetic states. (B) The final results of simulations with spherocylinders and cylinders or AR=1 or AR=2 and a range of binding interaction energy (y-axis).<sup>89</sup> Adapted with permission from reference #89. Copyright 2011 American Chemical Society.

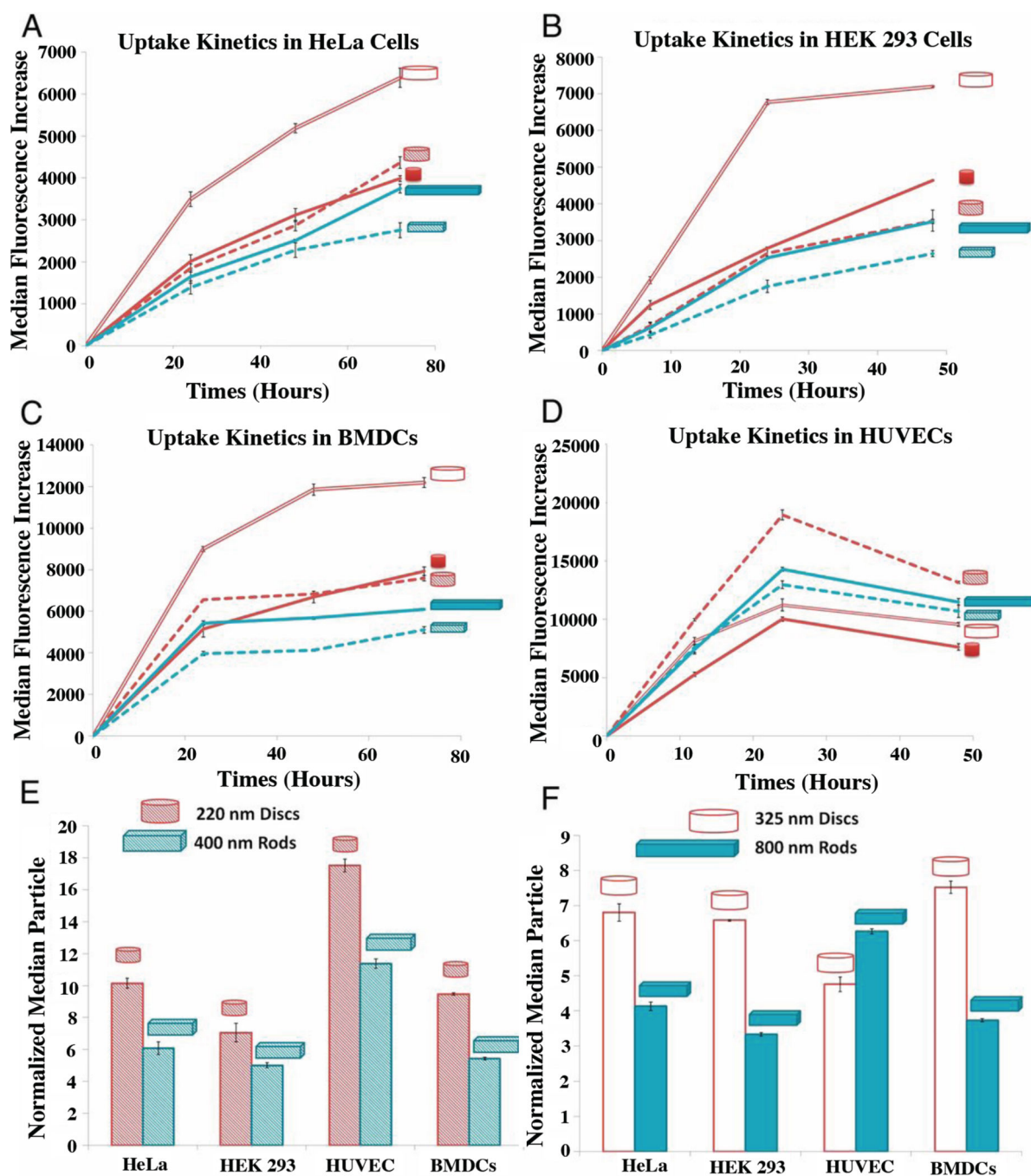


**Figure 10.**

Cellular-uptake kinetics of different shape-specific NPs in various cell lines. (A) HeLa cells, (B) HEK 293 cells, (C) BMDCs, and (D) HUVEC cells. (E–F) Normalized particle uptake per cell at maximal internalization time point.<sup>97</sup> Reproduced with permission from reference #97. Copyright 2013 National Academy of Sciences, U.S.A.

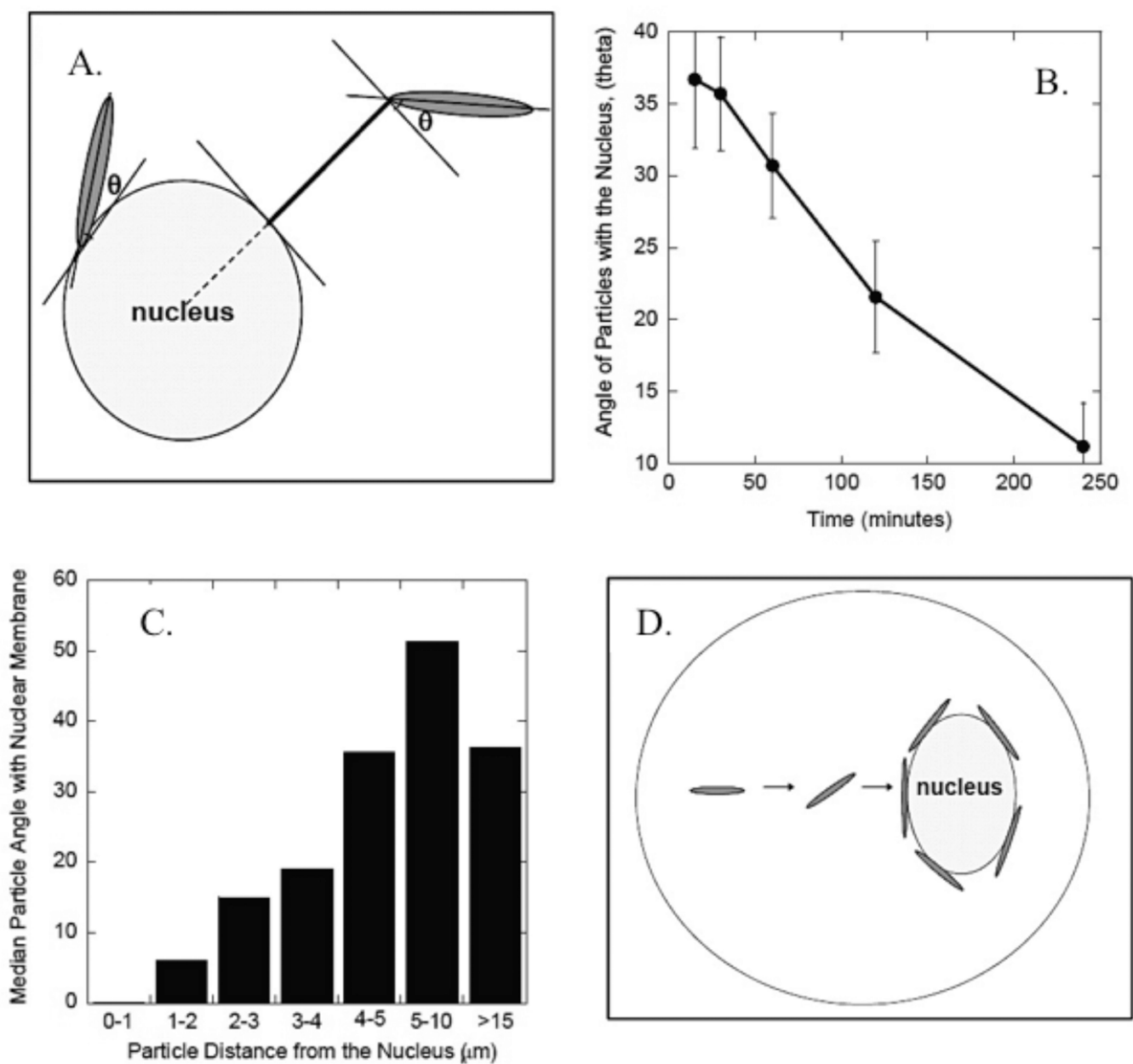


**Figure 11.**

Alignment of Poly(lactide-*co*-glycolide) particles with cell nuclei after internalization. (A) Schematic of angle,  $\theta$ , made between elliptical disk and nuclear membrane, (B) the dependence of  $\theta$  on time, (C) the relationship between  $\theta$  and distance from nucleus, and (D) a schematic of intracellular particle movement.<sup>95</sup> Reproduced with permission from reference #95. Copyright 2010 John Wiley & Sons, Inc.

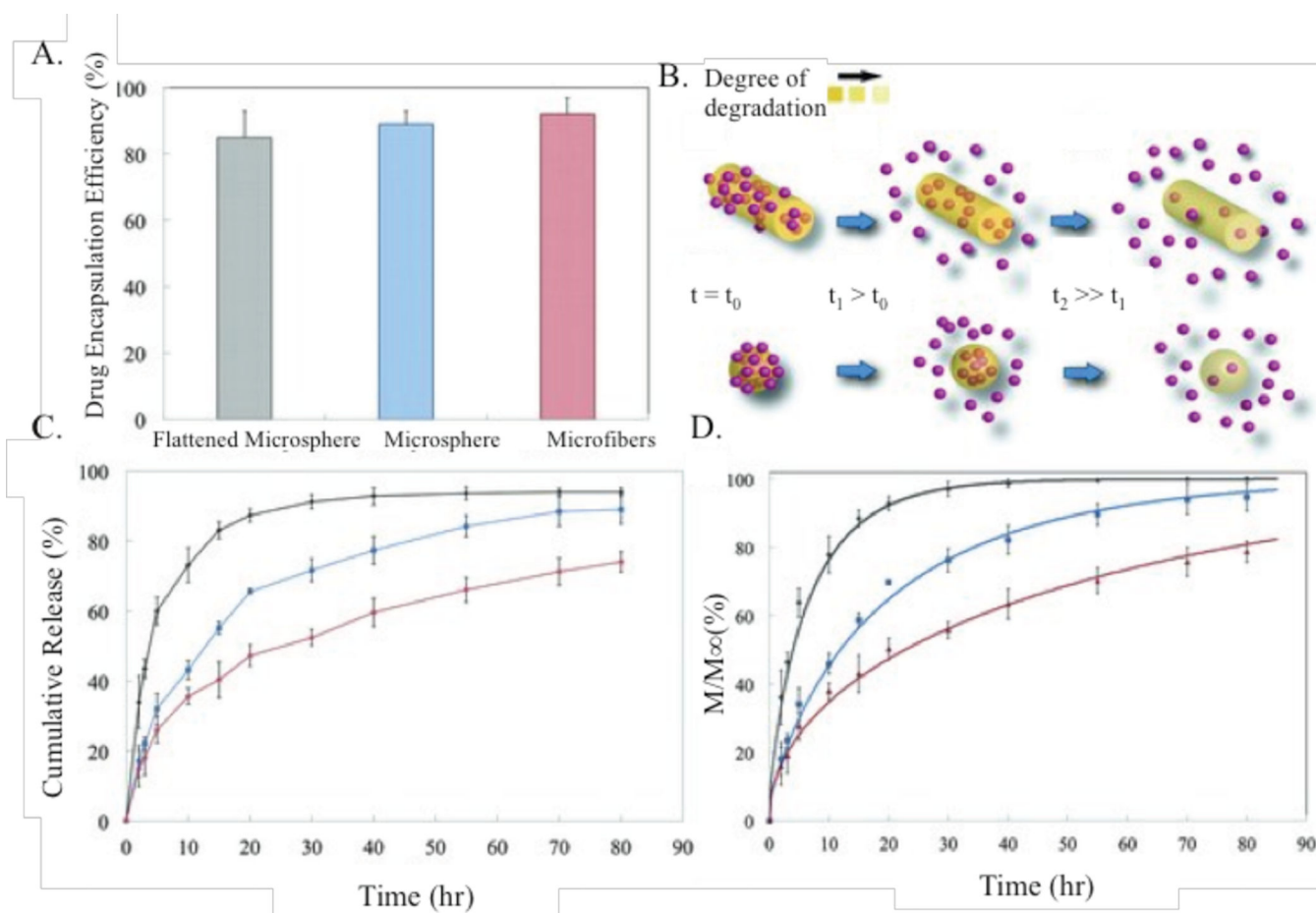


**Figure 12.** Drug release profiles of differently shaped PLGA particles. (A) encapsulation efficiency of varying shapes, (B) schematic representation of degradation of microspheres and microfibers over time, (C) the resulting dependence of release profiles on shape, and (D) mathematical modeling of same processes as in (C).<sup>110</sup> Reproduced with permission from reference #110. Copyright 2013 John Wiley & Sons, Inc.

**Table 1**

Critical ARs and wrapping time dependence on particle volume. (A) gives the spherical radius; particle volume is held constant for each row. Column (B) provides the AR for which complete wrapping requires minimal time, column (C) gives the fastest half wrapping time of internalization, (D) provides the lower critical AR, and (E) gives the upper critical AR.<sup>90</sup> Reproduced with permission from reference #90. Copyright 2008 Elsevier.

A	B	C	D	E
$R_s$ [nm]	$\Gamma$	$0.5\tau_w$ [s]	$\Gamma'_{cr}$	$\Gamma'_{cr}$
38.35 (= $R_{min}$ )	1	$\infty$	1	1
50	1.055	42.48	0.84	1.19
75	1.001	95.3	0.64	1.56
100	1.003	169.45	0.53	1.89
150	1	381.15	0.4	2.48
300	0.996	1524.6	0.25	3.94
500	1	4235	0.18	5.54